THE JOURNAL OF COMPARATIVE NEUROLOGY 497:959–980 (2006)

Focal Projections of Cat Auditory Cortex to the Pontine Nuclei

MERCEDES PERALES,[1] JEFFERY A. WINER,[2] AND JORGE J. PRIETO[1]*
[1]Department of Histology and Anatomy, University Miguel Hernandez, 03550 — Sant Joan d'Alacant, Spain
[2]Division of Neurobiology, Department of Molecular and Cell Biology, University of California at Berkeley, Berkeley, California 94720-3200

ABSTRACT

The pontine nuclei (PN) receive projections from the auditory cortex (AC) and they are a major source of mossy fibers to the cerebellum. However, they have not been studied in detail using sensitive neuroanatomical tracers, and whether all AC areas contribute to the corticopontine (CP) system is unknown. We characterized the projection patterns of 11 AC areas with WGA-HRP. We also compared them with their corticothalamic and corticocollicular counterparts. A third objective was to analyze the structure of the CP axons and their terminals with BDA. Both tracers confirm that all AC areas projected to lateral, central, and medial ipsilateral pontine divisions. The strongest CP projections were from nontonotopic and polymodal association areas. Preterminal fibers formed single terminal fields having many boutons en passant as well as terminal endings, and there was a specific morphological pattern for each pontine target, irrespective of their areal origin. Thus, axons in the medial division had a simpler terminal architecture (type 1 terminal plexus); both the central and lateral pons received more complex endings (type 2 terminal plexus). Auditory CP topographical distribution resembled visual and somatosensory CP projections, which preserve retinotopy and somatotopy in the pons, respectively. However, the absence of pontine tonotopy suggests that the AC projection topography is unrelated to tonotopy. CP input to the medial and central pons coincides with the somatosensory and visual cortical inputs, respectively, and such overlap might subserve convergence in the cerebellum. In contrast, lateral pontine input may be exclusively auditory. J. Comp. Neurol. 497:959–980, 2006.

Indexing terms: corticopontine; auditory system; axons; cerebellum; corticofugal projections

Understanding the roles of the auditory corticofugal system has been an important theme, since these massive projections can affect many aspects of hearing, including frequency specific tuning (Winer et al., 1998, 2001; Suga et al., 2000; Yan and Ehret, 2001; Hazama et al., 2004), receptive field architecture (Xiao and Suga, 2002), and ascending information flow (Weedman and Ryugo, 1996; Winer et al., 1998, 2001; Coomes and Schofield, 2004; Schofield and Coomes, 2005), to name just a few. In spite of the fact that corresponding corticofugal auditory projections to the pontine nuclei (PN) have been known for many years and documented in several species (Kusama et al., 1966; Diamond et al., 1969; Brodal, 1972c, 1983; Chiba, 1980; Wiesendanger and Wiesendanger, 1982a,b; Giménez-Amaya, 1988; Legg et al., 1989; Lee and Mihailoff, 1990; Schmahmann and Pandya, 1991; Knowlton et al., 1993; Glickstein, 1997), their neuroanatomical organization has received sparse attention with the most sensitive contemporary axoplasmic tracers, and their role in auditory function remains elusive. The present study addresses the nature of these projections with regard to auditory cortex (AC). More specifically, we ask whether each AC subdivision has such a projection, whether it is topographic, whether the patterns of projection from primary, nonprimary, and limbic-related cortex are distin-

Grant sponsor: National Institutes of Health; Grant number: R01 DC02319-26.

*Correspondence to: Jorge J. Prieto, M.D., Ph.D., Department of Histology and Anatomy, University Miguel Hernandez, Carretera Alicante-Valencia N332, s/n, 03550 — Sant Joan d'Alacant, Spain.
E-mail: m.perales@umh.es

Received 25 July 2005; Revised 1 December 2005; Accepted 30 December 2005

DOI 10.1002/cne.20988

Published online in Wiley InterScience (www.interscience.wiley.com).

guished, if any AC projections overlap in the pons with those from other modalities, and how the corticopontine (CP) preterminal fibers are organized in the PN. The answers to these questions could encourage more explicit physiological and functional hypotheses about the roles of this system.

The cortical projections to the PN embody convergence and divergence. Thus, input from the entire sensory neocortex converges on these comparatively small nuclei, and their few neurons, in turn, project as mossy fibers that divide and terminate in much of the cerebellar cortex. This transformation from a focal to a highly divergent projection pattern would seem unnecessary if the PN served only to relay AC information to the cerebellum, whereas the segregation and convergence of cortical information from many regions prior to its cerebellar redistribution would seem more congruent with modern theories of cerebellar function (Brodal and Bjaalie, 1992).

The CP connections arise from many neocortical regions, some having specific patterns of projections (visual: Brodal 1972a,b; Albus et al., 1981; Bjaalie and Brodal, 1983, 1989; Bjaalie, 1985, 1986, 1989; Bjaalie and Diggle, 1990; Bjaalie et al., 1997; somatosensory: Brodal, 1968a,b; Overby et al., 1989; Bjaalie et al., 1997). Auditory CP projections have been documented in the rat (Wiesendanger and Wiesendanger, 1982a,b; Legg et al., 1989; Lee and Mihailoff, 1990), monkey (Schmahmann and Pandya, 1991; Glickstein, 1997), rabbit (Knowlton et al., 1993), and cat (Kusama et al., 1966; Diamond et al., 1969; Brodal, 1972c, 1983; Chiba, 1980; Giménez-Amaya, 1988). In the cat, degeneration studies showed a CP projection after lesions in the primary AC (AI), the second AC (AII), and the posterior ectosylvian gyrus (Ep) (Brodal, 1972c). AC input was apparently confined to the dorsolateral PN, a finding confirmed in later anterograde tract-tracing studies in the auditory region of the anterior ectosylvian sulcus (Giménez-Amaya, 1988). However, a single tracer injection in rat primary auditory cortex (Te1) (Wiesendanger and Wiesendanger, 1982b) produced discontinuous patches of anterograde labeling in some pontine regions, suggesting that the AC input may target discrete groups of neurons. This implies that prior degeneration or autoradiographic studies in the cat may not have revealed this projection fully.

There are reasons to predict that projections from different AC areas may differ qualitatively and/or quantitatively. In the cat, 12 AC areas have been identified by connectional and/or electrophysiological techniques. Tonotopic (primary) areas include AI, and the anterior (AAF), posterior (P), and ventroposterior (VP) fields (Merzenich et al., 1975; Knight, 1977; Reale and Imig, 1980; Phillips and Irvine, 1982; Phillips and Orman, 1984). Association (nonprimary) areas comprise the secondary auditory area (AII), the dorsal auditory zone/suprasylvian fringe (DAZ), and the dorsal (EPD), intermediate (EPI), and ventral (EPV) parts of the posterior ectosylvian gyrus (Schreiner and Cynader, 1984; Winer, 1992; He and Hashikawa, 1998). Finally, limbic/polymodal association areas include the anterior ectosylvian sulcus (AES), and the insular (Ins) and temporal (Te) cortices (Woolsey, 1960, 1961; Sindberg and Thompson, 1962; Avanzini et al., 1969; Fallon and Benevento, 1977; Fallon et al., 1978; Shinonaga et al., 1994; Clascá et al., 1997). Connectional studies show that each area has a particular pattern of connections with the medial geniculate body (MGB; Niimi and Matsuoka, 1979; Roda and Reinoso-Suarez, 1983; Imig and Morel, 1984, 1985; Morel and Imig, 1987; Rouiller et al., 1989; Brandner and Redies, 1990; Clarey and Irvine, 1990b; Bajo et al., 1995; Clascá et al., 1997; Huang and Winer, 2000; Winer et al., 2001; Kimura et al., 2003), the

Abbreviations

AAF	anterior auditory field
AES	anterior ectosylvian sulcus
AI	primary auditory cortex
AII	second auditory cortex
BIC	brachium of the inferior colliculus
CC	caudal cortex of the inferior colliculus
CG	central gray
CIC	commissure of the inferior colliculus
CN	central nucleus of the inferior colliculus
cp	cerebral peduncle
CS	superior central nucleus
D	dorsal nucleus of the medial geniculate body
DAZ	dorsal auditory zone/suprasylvian fringe
DC	dorsal cortex of the inferior colliculus
DCN	dorsal cochlear nucleus
EPD	posterior ectosylvian gyrus, dorsal part
EPI	posterior ectosylvian gyrus, intermediate part
EPV	posterior ectosylvian gyrus, ventral part
FIC	fissure intercomissural
FL	flocculus of the cerebellum
GCL	cochlear nucleus granular cell domain
I-X	cerebellar lobules
IcT	intercollicular tegmentum
Ins	insular cortex
IPA	apical interpeduncular nucleus
IPC	central interpeduncular nucleus
IPO	posterior interpeduncular nucleus, outer division
IPP	paramedian interpeduncular nucleus
LGB	lateral geniculate body
LN	lateral nucleus of the inferior colliculus
M	medial division of the medial geniculate body
MCP	middle cerebellar peduncle
P	posterior auditory field
PFL	paraflocculus of the cerebellum
PML	paramedian lobule of the cerebellum
PVCN	posteroventral cochlear nucleus
RP	rostral pole nucleus of the inferior colliculus
RR	retrorubral field
Sa	sagulum
SC	superior colliculus
SGI	stratum griseum intermediale
SgL	suprageniculate nucleus, lateral part
SgM	suprageniculate nucleus, medial part
SGP	stratum griseum profundum
SGS	stratum griseum superficiale
SI	primary somatosensory cortex
SII	second somatosensory area
SIV	fourth somatosensory area
SN	substantia nigra
Te	temporal cortex
TRC	tegmental reticular nucleus, central division
TRP	tegmental reticular nucleus, pericentral division
V	ventral division of the medial geniculate body
VP	ventral posterior auditory field
Planes of section:	
A	anterior
D	dorsal
L	lateral
M	medial
P	posterior
R	rostral
V	ventral

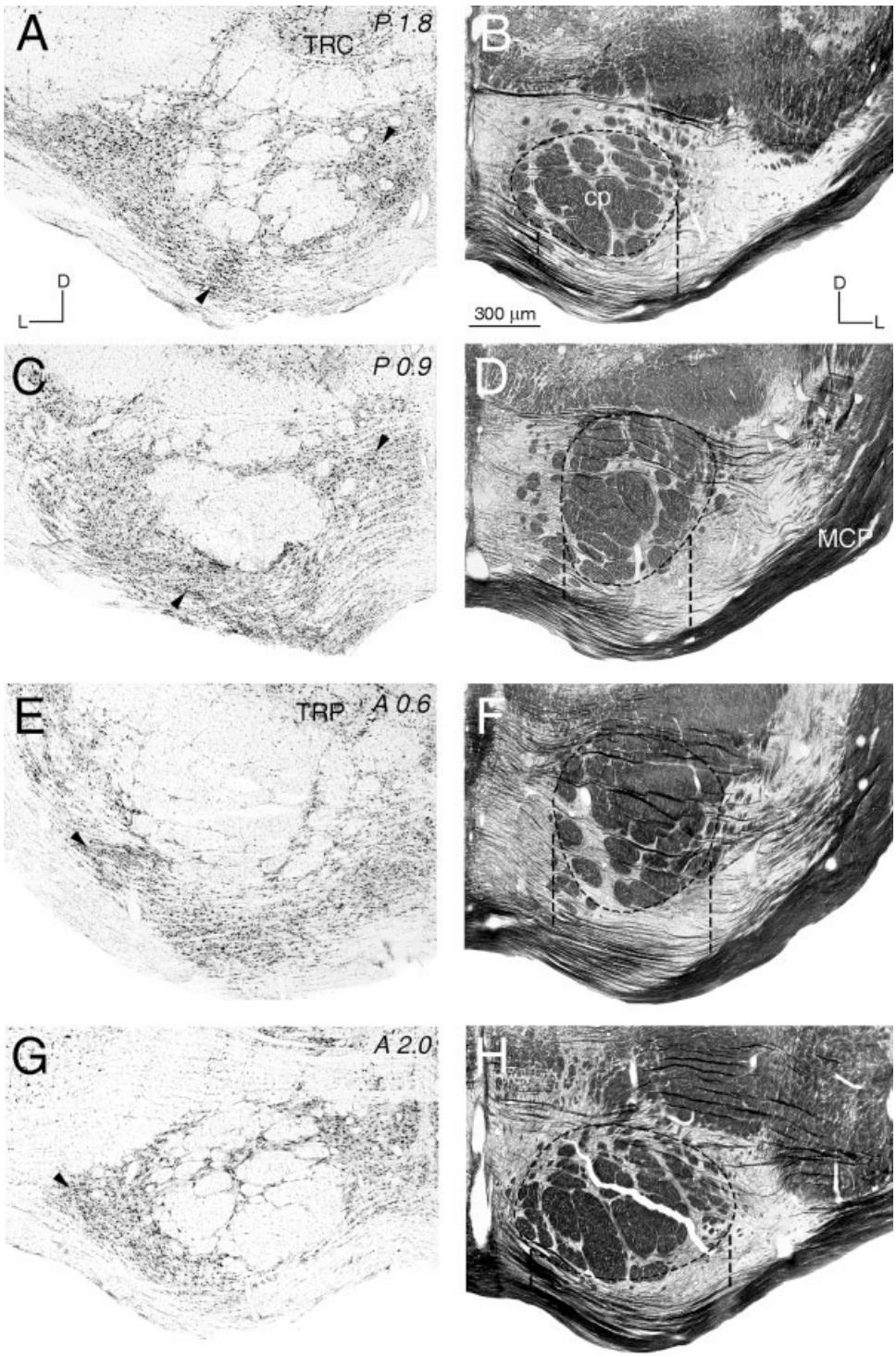

Fig. 1. Cyto- and myeloarchitecture of the pontine nuclei (PN) in pairs of matched sections midway through the pons. **A,C,E,G:** Nissl preparations. The PN extend rostrocaudally for about 6 mm (stereotaxic levels A3.0 to P3.0). Specific nuclei within the pons were not recognized. Arrowheads: clusters of large neurons that extended caudorostrally. **B,D,F,H:** Corresponding myelin stained preparations. Osmicated, epoxy-embedded whole-mounts 100 μm thick. Bridges of gray matter link the medial and lateral PN regions, crisscrossing the corticospinal axons that shape the cerebral peduncle (the oval profile). Vertical dashed lines mark the limits between the central, medial, and lateral pontine regions defined by reference to the cerebral peduncle. For abbreviations, see list.

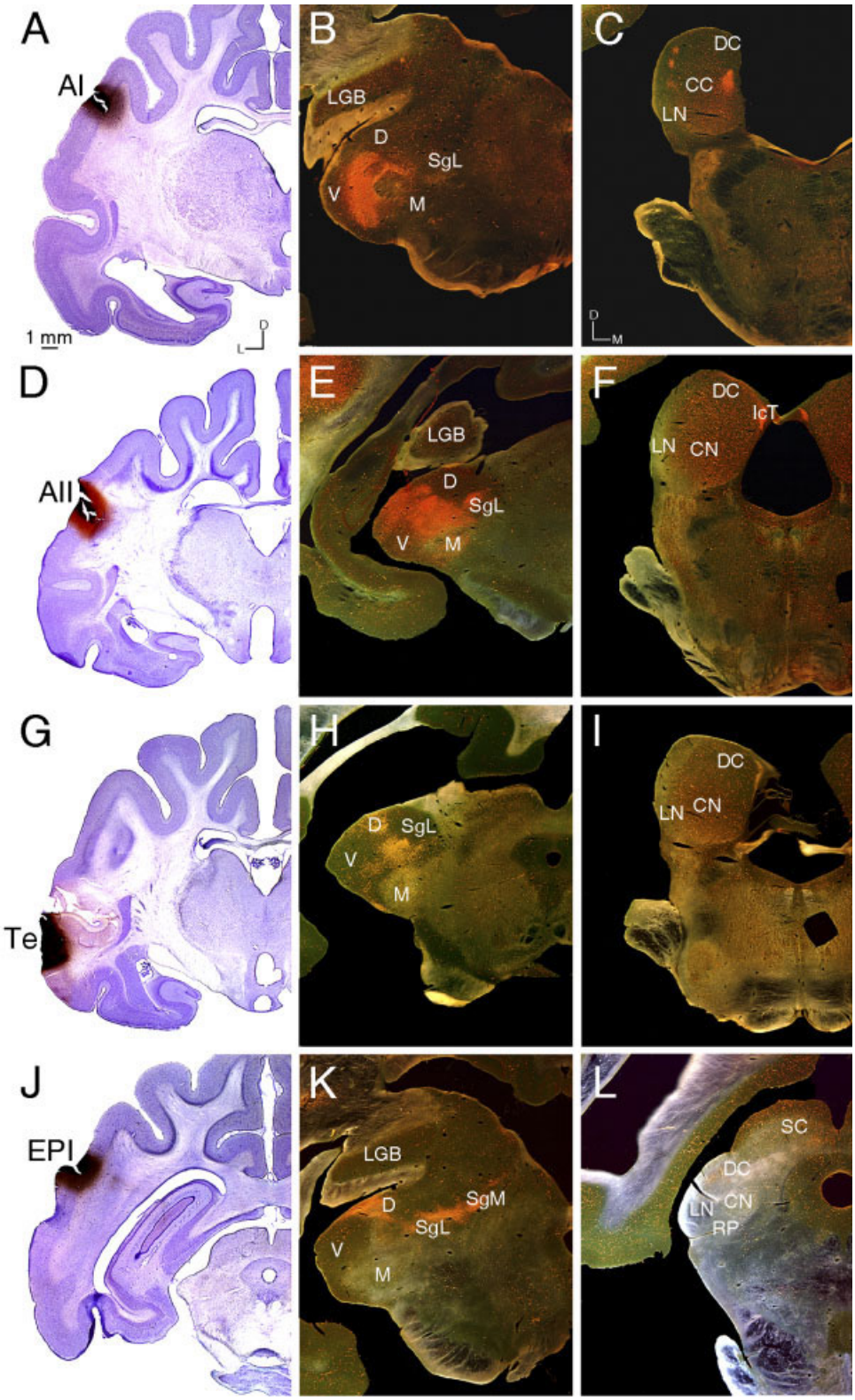

Fig. 2. Micrographs of the injection of WGA-HRP deposit sites in some AC subdivisions (**A,D,G,J**). The DAB-reacted sections, counterstained for Nissl substance, were used to determine the boundaries of the injection sites and to identify cortical areas. The other panels show the respective projections to the medial geniculate body (MGB; **B,E,H,K**) and the inferior colliculus (IC; **C,F,I,L**) similar to previously published results (Winer et al., 1998, 2001) and were used to confirm the locus of the cortical injection. For abbreviations, see list.

TABLE 1. Summary of Experiments

Area injected	Experiment	Tracer	Volume	Survival (days)	Figures
AI	1217	5% WGA-HRP	1.2 μl	4	1A–C, 3
AI (caudal)	46	5% WGA-HRP	0.6 μl	3	
AI	1382 left	20% BDA	1.32 μl	6	
AAF	1219	5% WGA-HRP	0.66 μl	3	
AAF	1381 right	20% BDA	0.88 μl	7	10B, 11A
P	1222	5% WGA-HRP	0.45 μl	3	
P	105	5% WGA-HRP	0.88 μl	4	
P	1361	20% BDA	0.88 μl	8	
VP	1317	5% WGA-HRP	0.23 μl	3	
VP	1358	20% BDA	0.8 μl	8	
DAZ	44	5% WGA-HRP	0.8 μl	3	
DAZ	1380 left	20% BDA	2.07 μl	6	11B
AII	1218	5% WGA-HRP	0.6 μl	4	1D–F, 4
AII	1301	10% BDA	Iontophoresis	20	
EPD	23	5% WGA-HRP	0.6 μl	4	5
EPD	1371 left	20% BDA	0.88 μl	6	
EPI	45	5% WGA-HRP	0.6 μl	3	1J–L, 6
EPI	1312	5% WGA-HRP	0.2 μl	3	
EPV	1313	5% WGA-HRP	0.2 μl	3	
Te	1224	5% WGA-HRP	0.6 μl	4	1G–I, 7
Te	1364	20% BDA	0.88 μl	7	
Ins	42	5% WGA-HRP	0.45 μl	3	8
Ins	1381 left	20% BDA	1.2 μl	7	10A, 11C

WGA-HRP, wheat germ aggutinin-horseradish peroxidase; BDA, biotinylated dextran amines.

inferior colliculus (Cooper and Young, 1976; Andersen et al., 1980a,b; Winer et al., 1998), the claustrum (Reale and Imig, 1983; Beneyto and Prieto, 2001), and the sagulum (Beneyto et al., 1998). It would be surprising if the CP projections were less specific or orderly. The absence of a modern connectional study in the cat using sensitive tracers is the primary impetus for the present experiments.

The following questions were addressed: 1) Do all AC areas contribute to the CP projection and, if so, does each project equally? 2) Does an AC area project to more than one pontine subdivision? 3) Do the CP fibers from different AC areas converge? 4) Are projections from functionally affiliated AC areas convergent? 5) Is there topographic relations for overlap for AC inputs and those from visual and somatosensory areas?

A complementary question concerns the terminal structure of the AC corticofugal projections, since studies of the MGB (Rouiller and Ribaupierre, 1990; Bajo et al., 1995; Winer et al., 1999) and inferior colliculus (Cooper and Young, 1976; Andersen et al., 1980b; Winer et al., 1998) have each demonstrated diverse arrays of their preterminal fibers whose effects on postsynaptic neurons might well differ. This diversity in the auditory CP system may have also different functional implications for their targets.

MATERIALS AND METHODS

Surgical procedures

The experiments were performed in Spain and in the United States. All experimental procedures followed approved institutional animal care and use protocols and the provisions enumerated in the National Institutes of Health guidelines. Adult cats of either sex, free from middle ear infection and with a normal Preyer's reflex, were used. Sodium pentobarbital (40 mg/kg, intraperitoneal, i.p.) was given for anesthesia before surgery or perfusion. The animal's anesthetic status was monitored continuously and maintained at physiologically appropriate levels. After corneal and pedal reflexes were abolished, the animal was placed in a stereotaxic head holder and a craniotomy exposed the AC. Targets were located by sulcal landmarks related to electrophysiological and anatomical investigations (Reale and Imig, 1980).

We analyzed the projections from 11 of the 12 auditory cortical areas, excluding area AES, which lies in the depth of the sulcus, and whose limits are variable, making electrophysiological identification indispensable for its precise location (Sindberg and Thompson, 1962; Clarey and Irvine, 1986, 1990a,b). Twenty-three hemispheres with injections confined to one architectonic field were available (Table 1). For topographical analysis we used unilateral injection of wheat germ agglutinin conjugated to horseradish peroxidase (WGA-HRP; 5% in sterile water; Sigma, St. Louis, MO) made by pressure through a glass pipette (tip diameter, 20–40 μm) coupled to a nanoliter hydraulic injector (World Precision Instruments, Sarasota, FL). A second series of experiments used biotinylated dextran amines (BDA 10–20%, 3 K m.w.; Molecular Probes, Eugene, OR) in glass pipettes by pressure (dissolved in distilled water) or iontophoresis (tracer in normal saline). Since BDA bulk-fills axons by diffusion in a Golgi-like manner (Brandt and Apkarian, 1992), it allowed us to classify the CP preterminal fibers, including their terminal boutons, and to confirm the WGA-HRP studies independently.

Histological procedures

After a 2–4-day survival, the WGA-HRP animals were perfused intracardially with washout (0.1 M phosphate buffer [PB], pH 7.4, the vehicle for all solutions, and 0.02% lidocaine hydrochloride, 250–400 ml total) that preceded initial fixation (0.5% glutaraldehyde/0.5% paraformaldehyde/PB, 1,000 ml), followed by 1.5% glutaraldehyde/1% paraformaldehyde (PB, 2,000 ml). After 1–2 hours, the fixative was replaced with cryoprotectant (10% sucrose/PB). Tissue was frozen-sectioned serially at 60 μm with a sliding microtome and several series of sections were reacted with tetramethylbenzidine (TMB; Mesulam, 1978) to reveal the anterogradely labeled axon terminals, then counterstained lightly with neutral red for cytoarchitectonic analysis. After

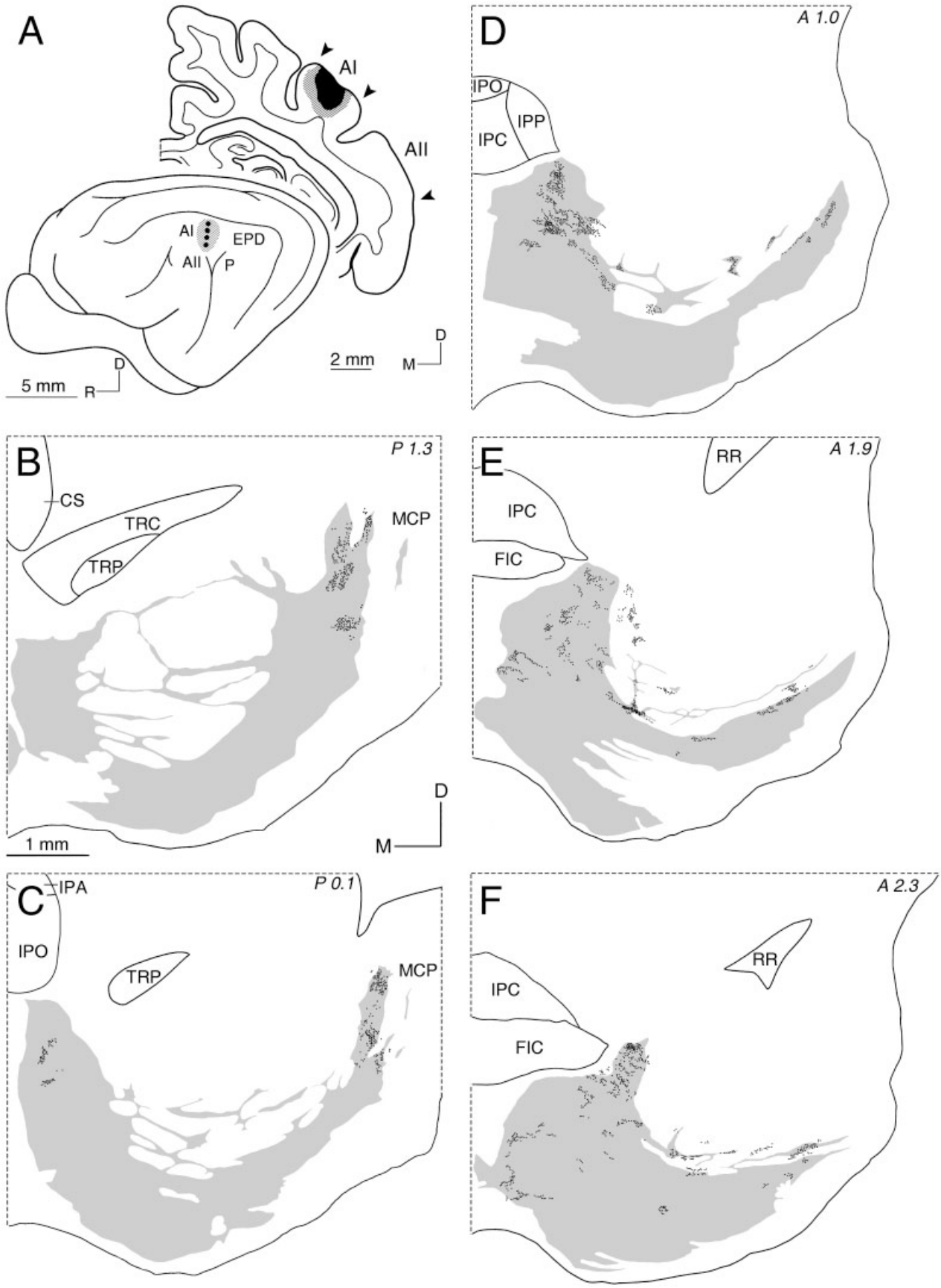

Fig. 3. PN projections from area AI. **A:** Lateral and transverse views of the left hemisphere. Black, center of the WGA-HRP deposit; stipple, tracer diffusion; drawing from Figure 2A. Four WGA-HRP deposits filled most of the central part of AI. Arrowheads: borders. **B–F:** Rostrocaudal series of representative coronal sections. Fine stippling represents axonal terminal fields of anterogradely transported WGA-HRP revealed with TMB. Gray stippled represents the perimeter of PN. AI injections labeled moderate clusters of axons in the lateral and medial PN. Sparse labeling was also present in the central region abutting the pyramidal tract. Numbers (top right) are the stereotaxic anteroposterior level.

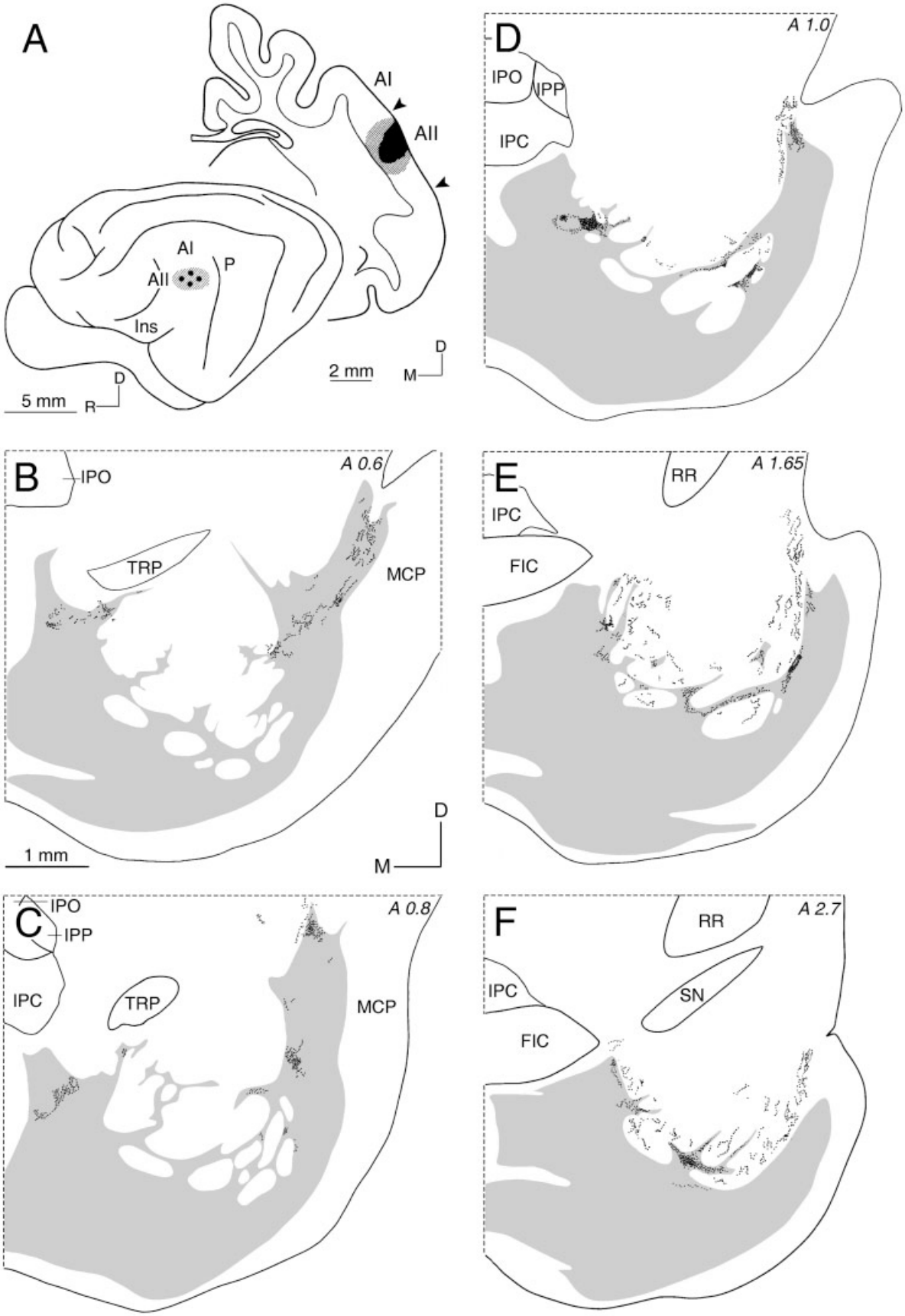

Fig. 4. AII projections to the PN. **A:** Four WGA-HRP injections were confined to AII. **B–F:** The dense labeling was concentrated in the lateral (caudally), medial, and central (rostrally) PN. There was a striking mass of axon terminals in the medial pons (A1.0; panel D) resembling that found in the same stereotaxic level after AI deposits (Fig. 3D).

locating the injection site in the TMB material, adjacent, untreated sections were incubated with nickel/cobalt-intensified diaminobenzidine (DAB; Adams, 1981) to more accurately view its size. Unreacted sections were Nissl stained.

In the BDA experiments, animals were reanesthetized after 7–10-day survivals and perfused as above except with 4% paraformaldehyde. The tissue was cryoprotected in 30% sucrose and 50-μm-thick frozen sections were cut, incubated in the ABC Elite reagent (Vector Laboratories, Burlingame, CA), and followed by nickel-cobalt intensified DAB treatment.

Data analysis

TMB-reacted sections counterstained with neutral red were used to draw architectonic borders and to plot anterogradely labeled axon terminal fields. Sections with representative patterns of anterograde labeling were selected for presentation and the locus of axons drawn at 125×, under darkfield illumination, through a drawing tube. The estimations of the strength of the anterograde labeling are qualitative values, and they were derived by examining the intensity and extension of the plots in all the sections with CP projections. The analysis was done by two viewers independently.

The MGB was processed to demonstrate the thalamocortical cells of origin. This served as an independent check on the cortical injection site, since each AC area has a unique pattern of thalamic input (Niimi and Matsuoka, 1979; Imig and Morel, 1984, 1985; Morel and Imig, 1987; Brandner and Redies, 1990; Clarey and Irvine, 1990b; Clascá et al., 1997; Huang and Winer, 2000; Winer et al., 2001; Kimura et al., 2003). Architectonic borders were drawn without reference to the CP labeling and we selected for the CP studies only experiments in which both the distribution of thalamic labeled cells and the anterogradely labeled axon terminals matched precisely that of prior work. The analysis of the axon terminal labeling in the IC was also used to corroborate the CP results (Cooper and Young, 1976; Andersen et al., 1980a,b; Winer et al., 1998; Imig and Morel, 1985; Huang and Winer, 2000). Only experiments with deposits confined to the gray matter and remote from architectonic borders were accepted for subsequent analysis.

Many examples of BDA-filled axons and their preterminal fibers were drawn from each injection with a 100× oil immersion lens under brightfield illumination and through a drawing tube; the locus of labeling followed the distribution of WGA-labeled fibers. A digital camera (Nikon DXM1200 and ACT-1 camera control program, v. 2.11, Melville, NY) was used for photomicrography and the photos were later edited with Adobe Photoshop 7.0 (Adobe Systems, San Jose, CA). Editing did not alter the primary data in either form or content.

RESULTS

Cytoarchitecture

Prior studies recognized several PN on topographic, rather than cytoarchitectonic, grounds. Borders between the nuclei were arbitrary and inconsistent (Brodal and Jansen, 1946). Later work showed that the proposed subnuclei were similar cytoarchitectonically and that there was no systematic relationship between these architectonic subdivisions and their extrinsic connections (Brodal and Bjaalie, 1992). The scheme chosen here is therefore purely topographic and conceptually neutral, referring to the pontine areas in the transverse plane as medial, central, and lateral, relative to the ipsilateral cerebral peduncle.

The PN were prominent in Nissl (Fig. 1A,C,E,G) and corresponding osmicated (Fig. 1B,D,F,H) preparations for cyto- and myeloarchitecture, respectively. The PN are ~6 mm long (from stereotaxic levels A3.0 to P3.0) and are traversed horizontally by many fibers, especially dorsally. These axons formed part of the cerebral peduncle and they divided the thin bridges of interstitial gray matter joining the medial and lateral pontine regions. The bridges contained many densely packed neurons. Cytoarchitectonically, the medial, central, and lateral regions were heterogeneous: each had small, irregular, cell-rich areas, with some neurons densely packed or dispersed. Clusters of larger neurons (~15 × 20 μm in somatic diameter) were interspersed among more abundant small (~12 × 14 μm) neurons, and the large neurons were followed in consecutive sections, showing their caudorostral orientation (Fig. 1A,C,E,G: arrowheads).

Projections with WGA-HRP

Injection sites were ~2 mm or less in diameter, restricted to one AC area, and did not invade the white matter (Figs. 2A,D,G,J, 3A–8A). The position of the injection was compared with the retrograde and anterograde transport in the MGB (Fig. 2B,E,H,K) and with the anterograde pattern in the IC (Fig. 2C,F,I,L), and only those experiments with robust labeling confined to them were accepted for analysis of their CP projections. The terminal anterograde labeling was plotted from representative sections, excluding fibers of passage.

All AC areas projected to the PN, although the distribution of terminals was unique for each area. Results common to all experiments were: 1) each AC area projected to several pontine regions; 2) each pontine division received input from more than one AC area; 3) the lateral, medial, and central pons were labeled in every experiment, despite quantitative and qualitative differences; 4) axons arising from all the AC areas converged midway along the caudorostral pontine axis; 5) projections were ipsilateral, except for areas Ins and Te, which also projected contralaterally; 6) corticofugal projections from an AC area had a compartmental organization with small foci of PN terminals, some of which extended rostrocaudally; and 7) most lateral pontine labeling was caudal, whereas medial terminals were concentrated rostrally.

Tonotopic areas. For AI, we followed two strategies. In one experiment the tracer deposit was large enough to cover much of AI, and in another (not illustrated) the injection was restricted to caudal AI, whose cells prefer lower frequencies (Merzenich et al., 1975). These injections explored whether the AC CP projection was conserved across frequencies. The result in both experiments was topographically similar, suggesting CP convergence and a loss of frequency-specific organization, a finding in accord with prior work (Brodal, 1972c).

AI deposits labeled clusters of terminals in the lateral, central, and medial PN (Fig. 3). The most caudal sections (Fig. 3B,C) had labeling restricted to the lateral region, and formed dense foci. The lateral pons decreased in size rostral to A1.0 and, consequently, the afferents decreased

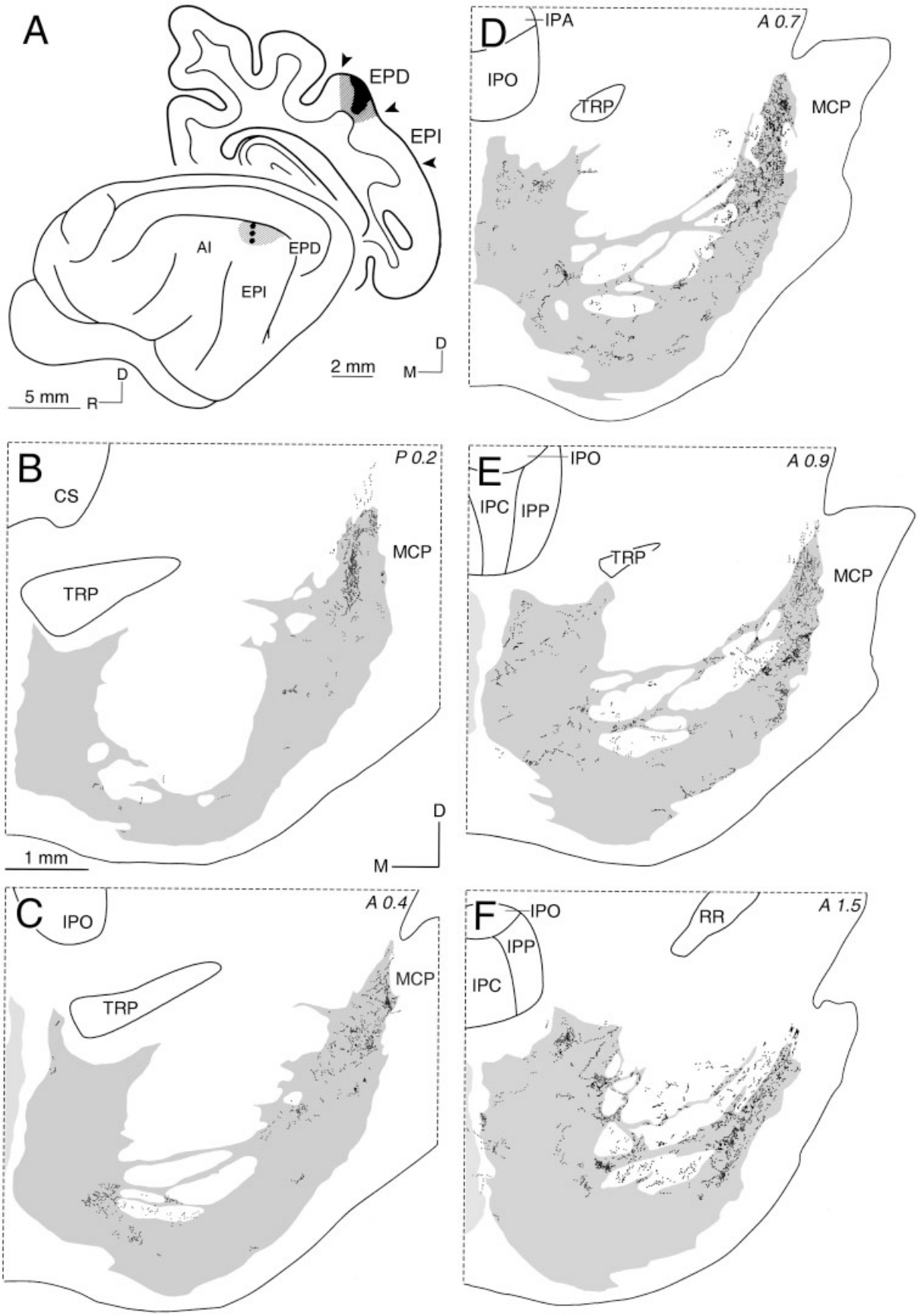

Fig. 5. **A:** Injections in EPD. **B–F:** The EPD labeling was far more widespread and farther from the pyramidal tract than that from AII deposits (Fig. 4); the strongest projection was to the dorsolateral PN.

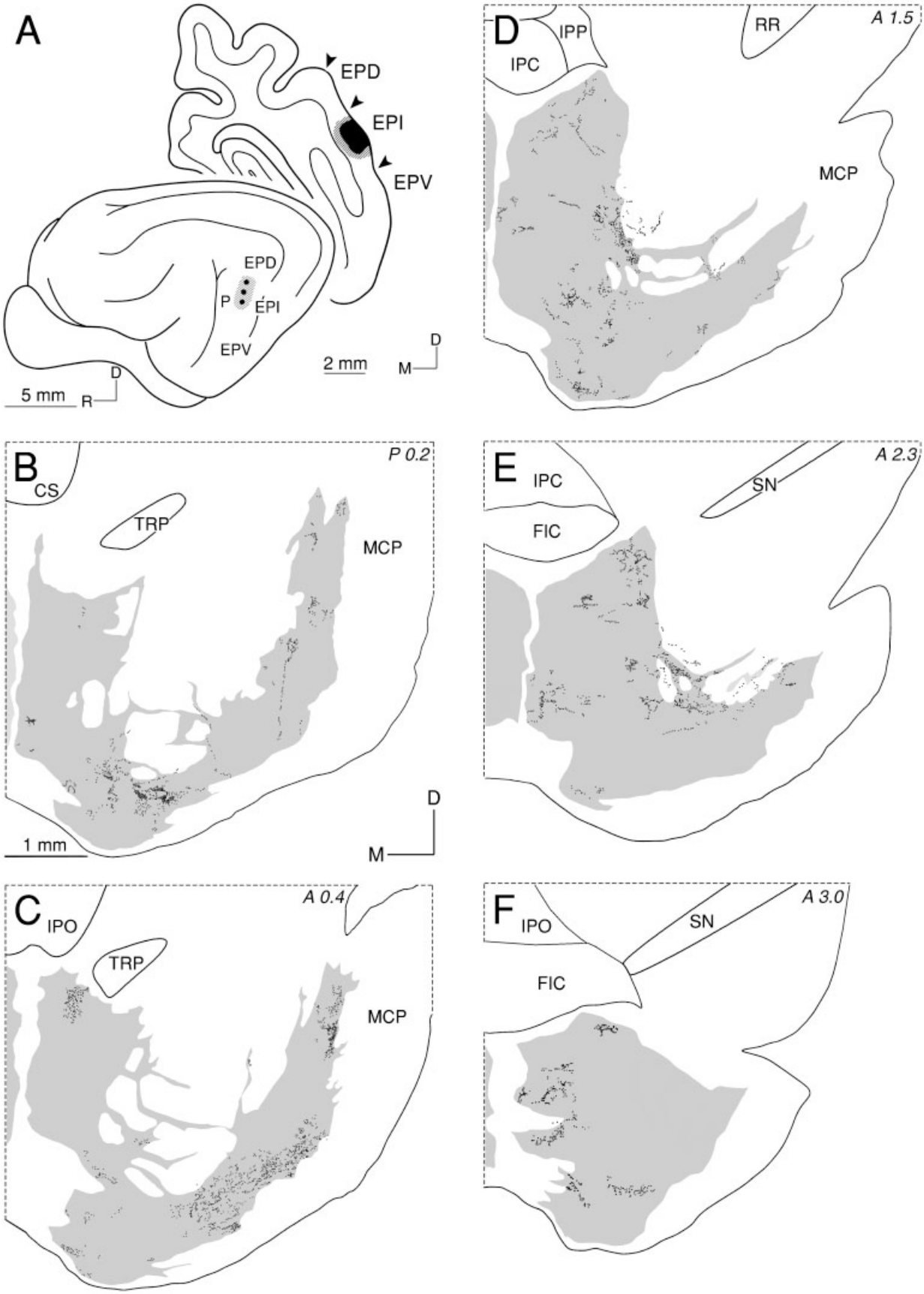

Fig. 6. **A:** Projections from EPI produced both focal and widespread PN labeling. **B–F:** The EPI labeling spanned all PN, and a striking feature was the caudal central pontine concentration of axonal terminals.

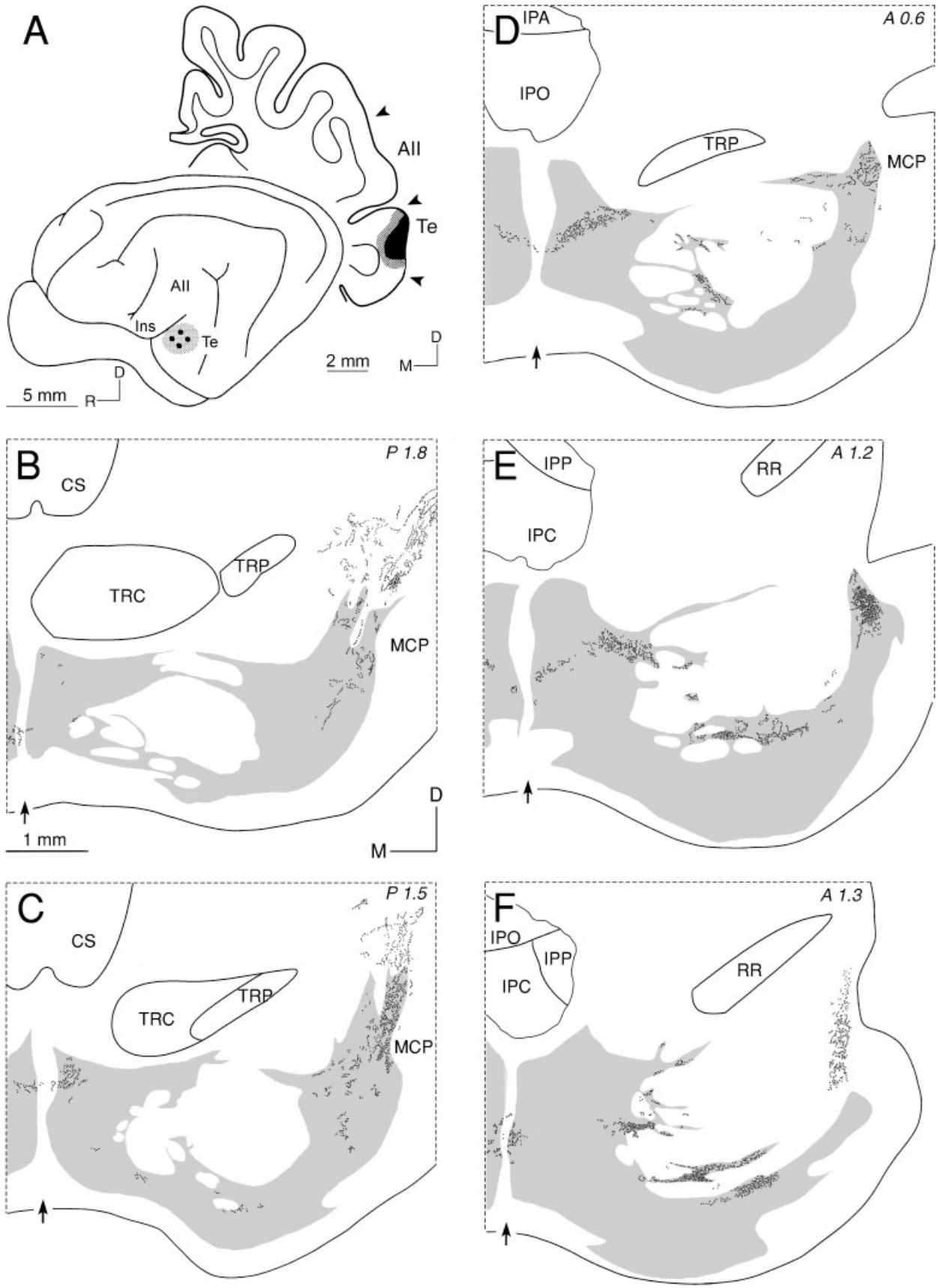

Fig. 7. **A:** PN labeling after WGA-HRP injections in the temporal cortex (Te), caudal to the pseudosylvian sulcus. **B–F:** Well-defined axonal terminal fields were found in the lateral, central, and medial pontine region, respectively. There was also contralateral pontine input (F). Arrows: the midline.

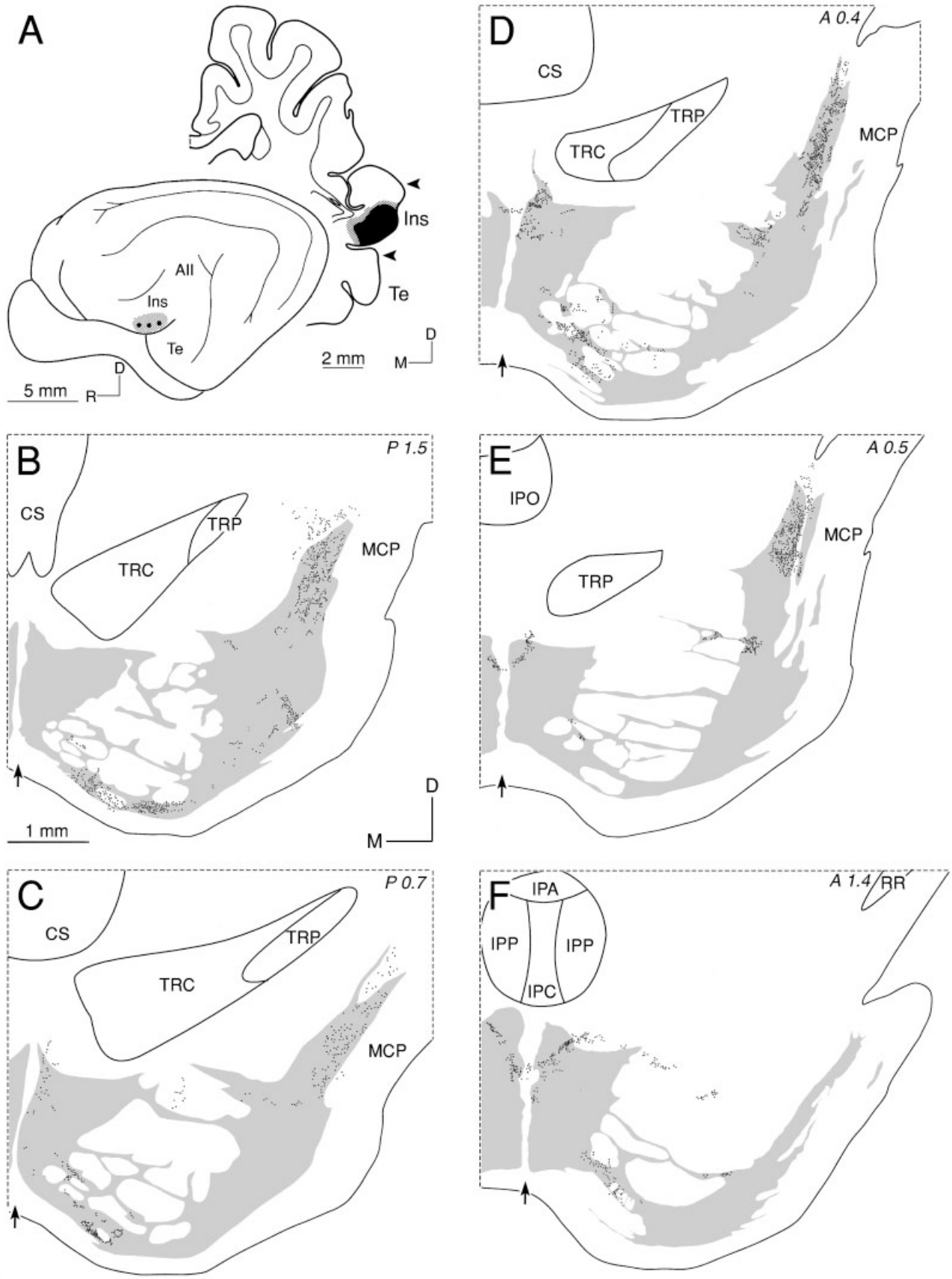

Fig. 8. Labeling from the insular cortex (Ins) to the pons. **A:** Coronal section of the injection site location and tracer diffusion. The tracer was limited to Ins, and the deposit did not enter the white matter. **B–F:** The distribution of labeling resembled that in area Te (Fig. 7), with terminal clusters segregated in the medial, central, and lateral PN, respectively, as well as the contralateral labeling near the midline.

progressively, while input to the central and medial pons increased (Fig. 3D–F). The CP fibers ending in the medial division formed several foci that were largest at A1.0 (Fig. 3D). Labeling more centrally was sparse and restricted to smaller, isolated terminal fields (Fig. 3D–F).

Projections from areas AAF, P, and VP are not illustrated since the distribution of labeling in each closely resembled the projection pattern described for AI deposits (Fig. 3). Nevertheless, the intensity of the CP labeling was slightly weaker and the foci of pontine axon terminals were more restricted.

Nonprimary auditory cortex. The AII CP projection (Fig. 4) resembled that for AI (Fig. 3): the labeling was in a similar rostrocaudal position (~P1.8–A2.2), the axon terminals were in the same pontine territory, and deposits in AI and AII both labeled dense foci in the medial pons at ~A1.0 (Figs. 3D, 4D). Features unique to the AII projection were the robust and dense input to the central pons rostrally, where it terminated in the slender gray matter bridges crossing the cerebral peduncle (Fig. 4E,F). Other intense terminal foci lay in the medial and lateral pons (Fig. 4C,D).

Unlike AII CP connections, those from areas EPD (Fig. 5) and EPI (Fig. 6) had different PN labeling patterns. In both instances labeling was widespread rostrocaudally and mediolaterally, and ranged from light and diffuse to moderate. Nevertheless, the EPI projection alone labeled the central pons in the most caudal sections (Fig. 6B), and these projections spanned nearly the entire rostrocaudal extent, being thus the most widespread in our series. EPD (Fig. 5) projected most strongly to the lateral pons and had the weakest input medially. Nevertheless, the rostrocaudal projection resembled that after AI and AII deposits, concentrating in the lateral pons caudally and in the central and medial territories more rostrally.

Polymodal areas. This Te and Ins projection was restricted to three large masses of labeling in the medial, central, and lateral pons, respectively. Te had the heaviest projection.

Te (Fig. 7) and Ins (Fig. 8) were unique in having a bilateral CP projection. Ipsilateral input to the medial pons was a massive, extended oblique band oriented dorsolaterally to ventromedially, whereas the contralateral pontine labeling was symmetrical, smaller, and lighter (Figs. 7C–F, 8E,F, left side).

In summary (Fig. 9), all AC areas project to lateral, medial, and central PN, and the distribution and density of the terminal fields was topographic. The rostrocaudal extent of input to the lateral PN (~P1.8–A0.6) was similar in all experiments, except in EPI, and the strongest projection arose from area EPD. In contrast, the rostrocaudal position of the central pontine labeling varied in each experiment. Thus, Ins, Te, and EPI alone projected to the caudal central division, whereas the other areas sent fibers rostrally, with AII having the heaviest input and AI the smallest. In the medial pons, the principal input was from AI, AII, and EPI, and the smallest from EPD, and in all experiments the labeling was concentrated preferentially in the anterior pons.

BDA labeling of corticopontine axons

These experiments confirmed the WGA-HRP results and permitted a morphological analysis of the auditory CP preterminal fields. Their terminal distribution was virtually identical with both tracers, although the lighter projections from WGA-HRP injections in areas AAF, P, and VP was pronounced in the BDA experiments. Cortical BDA deposits often labeled only one axon or a few pontine fibers in a section. Only representative types of terminal plexuses commonly encountered are described below.

BDA-filled CP axons crossed the ipsilateral cerebral peduncle to enter the PN; often, their preterminal fibers were restricted to one pontine subdivision, suggesting that restricted regions of an AC area projects to a particular PN area. Single axon trunks 1–2 μm thick formed elaborate terminal plexuses in the PN ending in cascades of finer fibers that often ran in parallel to the dendrites of unstained pontine neurons. Irrespective of their areal origin or PN location, the terminal plexuses had both en passant and terminal boutons, forming aggregates or located throughout the long and sinuous contours, and with up to 100 boutons labeled in a 25-μm expanse.

Moreover, there was a CP terminal projection pattern specific for a particular target. Fibers in the medial division formed lamellar arrays oriented dorsomedially. The BDA-filled axons entered ventrally and had a smooth preterminal trunk with a long intrapontine trajectory that turned abruptly before emitting a few, thin branches forming fascicles in neuropil-rich areas. They had a simpler terminal architecture (type 1 terminal plexuses) with some preterminal fibers running in straight line with few boutons along their trajectory (Fig. 10A:a) and as fibers with only terminal boutons (Fig. 10A:b). Terminal plexuses filled 50–80-μm-wide neuropil regions, and their boutons ranged from tiny (0.5 μm in diameter) to large (5 μm long by 2 μm wide).

The dorsolateral PN (Fig. 10B) received axons 1–3 μm thick dorsolaterally with single terminal fields represented by focal projections with many en passant and other terminal endings that divided profusely within territories 100–200 μm wide (Fig. 10B:c), and which are separated by bouton-free regions up to 40 μm long (type 2 terminal plexuses).

Preterminal fibers reaching the central pons near the cerebral peduncle differed from others because of the unique local architecture. Their terminal plexus overlapped the thin gray matter bridges among the cerebral peduncle axons. Preterminal fibers entered medially and divided in narrow fascicles up to 600 μm long and only 15 μm wide (Fig. 11A–C). Small or medium-sized boutons were concentrated in elongated, dense masses in the neuropil, with few terminals in proximity to neuronal somata, resembling the type 2 terminal plexuses in the dorsolateral PN (Fig. 11A:d).

DISCUSSION

Topographical corticopontine organization

All 11 areas of cat AC project to the PN, suggesting that auditory influence on the cerebellum may be larger than previously thought, and that the influence is heterogeneous both in origin and, prospectively, in function.

Prior work included few AC areas (AI, AII, and EP) and noted projections only to the dorsolateral PN (Brodal, 1972c; Chiba, 1980; Kawamura and Chiba, 1979; Broch-Smith and Brodal, 1990). We extend that result, documenting that all AC areas have CP projections to the dorsolateral PN and, moreover, that all AC areas also project to the central and medial PN, where they termi-

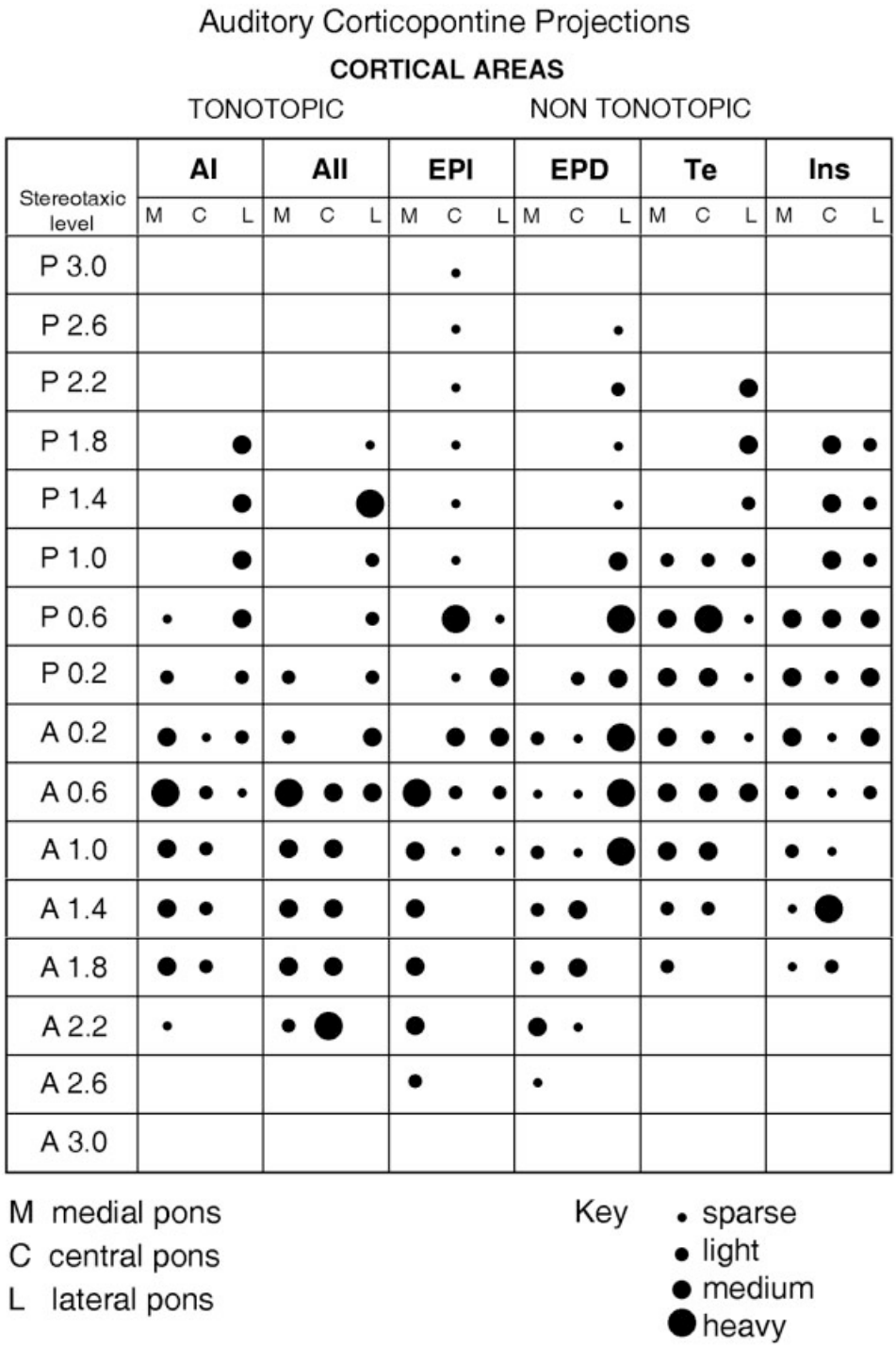

Fig. 9. Summary of the AC projections input to the PN. Upper line, origin of CP projections; lower line, PN targets of AC input. Left side, anteroposterior level. Dot size is proportional to the ipsilateral input strength (see key) and represents a qualitative assessment of CP labeling intensity and spatial distribution. The conclusions were that axon terminals from all AC areas 1) converged midway along the pontine caudorostral axis, 2) the lateral projections target the caudal pons preferentially, and 3) the medial inputs ended in the rostral pons.

nate in clusters. These results resemble those in rat (Wiesendanger and Wiesendanger, 1982b), and rabbit (Knowlton et al., 1993) and they are consistent with the distribution of c-fos expression after acoustic stimulation that activated several PN regions (Qian and Jen, 1994; Vischer et al., 1994).

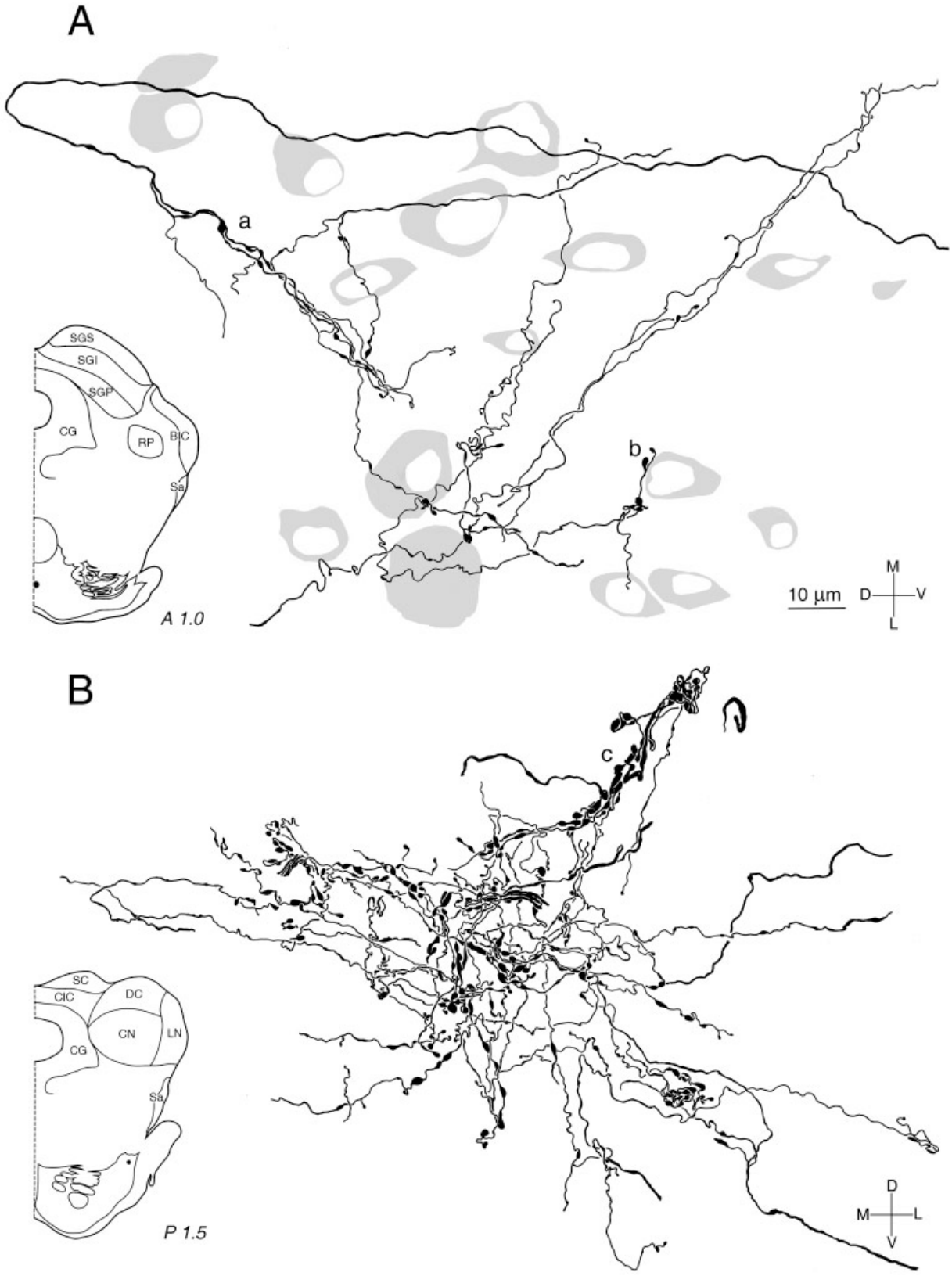

Fig. 10. Corticopontine terminals in the PN labeled by injection of BDA in Ins and AAF, respectively. **A:** An Ins deposit bulk-filled one axonal trunk in the medial PN that gave off a few, thin branches that ran parallel through neuropil-rich areas (type 1 terminal plexus). Some preterminal fibers had few boutons en passant (a) and others had only terminal boutons (b). Gray profiles, unstained somata viewed in Nomarski (differential interference contrast) optics. Dot in inset, the locus of the axon. **B:** A fiber plexus in the dorsolateral PN after an AAF injection. Two axon trunks divided profusely within discrete territories 100–200 µm wide, with many en passant boutons and terminal endings and separated by bouton-free regions. The elaborate plexus (c; type 2 terminal plexus) may run parallel to the primary dendrites of pontine neurons.

Auditory CP projections diverge strongly throughout the PN (Fig. 12), a pattern that suggests diverse spheres of CP influence. Thus, AI projects moderately to the lateral pons (caudally) and to the medial pons (rostrally). This implies that widely separated neuronal territories either receive common projections and have common functions, or that AI output itself targets different functional and architectonic pontine subdivisions. The present results cannot resolve this quandary, but the fact that all the fields have highly dispersed spatial pontine targets would seem to favor the second hypothesis. Resolution of this point will require joint physiological-anatomical studies in which the effects of AC stimulation are assessed in the pons, with conjoint exploration of the specific cerebellar territories that receive these influences. A second inference is that there is likely spatial overlap of the primary, nonprimary, and limbic-related acoustic input. Again, our experimental design is unsuitable to confirm this conclusion, but even casual inspection of the summary data (Fig. 9) is suggestive; the alternative view—that the projections from the different areas appear to converge but remain segregated synaptically—is equally appealing and will, again, require an approach that entails double anterograde labeling to demonstrate such convergence. In any event the AC pontine projection appears far more widespread and intricate in design than prior work suggests.

Studies of CP projections from other sensory cortices find patterns much like the present results. All areas of visual and somatic sensory cortex project to the PN, and the relative strength of each such areal projection is different and specific. Furthermore, visual and somatic sensory input forms patches and bands with rostrocaudal continuity and which are distributed throughout the PN (Brodal, 1968a,b, 1983; Brodal and Steen, 1983; Bjaalie and Brodal, 1989; Broch-Smith and Brodal, 1990). This feature suggests a degradation, or at least a superimposition by convergence, of cortical topography from each modality in the pons. However, in early development CP projections are organized differently: CP axons form a complex lamellar concentric pattern in the PN (Bjaalie et al., 1997), a pattern that preserves the simple topographic relation between the site of cortical origin and the location of the PN terminal fields (Leergaard et al., 1995). However, this pattern becomes obscured in mature animals by the postnatal retraction of some CP axons, transforming an otherwise continuous projection into an intricate mosaic of isolated patches and bands (Mihailoff et al., 1984; Bjaalie et al., 1997), much like that in the present study. Consequently, some fundamental principles of the CP system are conserved in all sensory modalities, including audition.

Is topographic information of the tonotopic areas conserved in the corticopontine projection?

The primary AC projections to the PN did not preserve the cortical topographic organization, and both global and restricted tracer injections in AI, and in other primary areas, produced similar labeling distributions that varied in density. This result is in close accord with experimental degeneration studies in which lesions in rostral or caudal AI produced much the same PN terminal distribution (Brodal, 1972c). Brodal proposed that AI CP projections, even though organized tonotopically, would be less precise than those of the corticocollicular or corticogeniculate projections (Diamond et al., 1969; Cooper and Young, 1976; Niimi and Matsuoka, 1979; Andersen et al., 1980a,b; Roda and Reinoso-Suarez, 1983; Imig and Morel, 1984, 1985; Morel and Imig, 1987; Rouiller et al., 1989; Brandner and Redies, 1990; Clarey and Irvine, 1990b; Bajo et al., 1995; Clascá et al., 1997; Winer et al., 1998, 2001; Kimura et al., 2003). A distinctive feature of AC organization (especially for areas AI, AAF, P, and VP) is a topographic arrangement of characteristic frequency, that is, the orderly arrangement across the cortical convexity. It is believed that the anatomical substrate conserving tonotopy along the auditory pathway is the precise organization of parallel ascending connections from each tonotopic nucleus to the subsequent structure. However, since such topographic preservation is absent in the AC CP projection, we infer that PN auditory-responsive neurons must not be organized tonotopically.

Moreover, a striking similarity of CP projections from AI (tonotopic area) and AII (nonprimary area) was seen in other studies describing projections to other premotor nuclei. Thus, whatever information that AI and AII convey to the pons, it cannot be solely related to tonotopic maps.

To verify whether the connectional results reflect a degraded topography, electrophysiological studies are essential. The only such study in cats that recorded from the PN during acoustic stimulation did not systematically explore all subdivisions (Aitkin and Boyd, 1978), as would be required to resolve the issue. However, studies in the bat find no tonotopic organization in any PN (Schuller et al., 1991; Kamada et al., 1992; Jen et al., 1993; Wu and Jen, 1995).

Work on the primary somatosensory and visual cortices showed that, unlike the auditory CP projection, there is a topographical distribution of CP input and, consequently, that somatotopy and retinotopy are preserved in the PN (Bjaalie, 1985, 1986; Overby et al., 1989; Leergaard et al., 2000; Leergaard, 2003). Thus, the auditory CP system is unusual since a point-to-point representation of the AC in the PN is not evident. Perhaps this organization is represented in several pontine regions, so that its topography within the PN would form a discontinuous map, recalling and resembling the fractured somatotopy in the spinocerebellar system (Shambes et al., 1978).

Axonal architecture

This is the first report on the light microscopic morphology of the auditory CP axons and boutons. Previous studies on the somatic sensory and visual CP axon terminals used electron microscopy only (Höllander et al., 1969; Mihailoff and King, 1975; Mihailoff et al., 1978; Mihailoff and Bourell, 1986), and considered the synaptic aspects of the CP terminals. Thus, they were unable to describe more global features of CP terminal organization such as their lamellar configuration or to document the terminal segregation and clustering as we did with BDA.

Only comparatively few AC neurons project to the pons, and their somata are dispersed in the cortex (Keizer et al., 1987). Moreover, the restricted tracer injections labeled very few pontine axons, although these branched robustly at their target. Many of the BDA deposits often labeled only one or two pontine axons trunks in a section, even when they produced far more abundant and widespread anterograde labeling in the auditory thalamus (Fig. 2B,E,H,K;

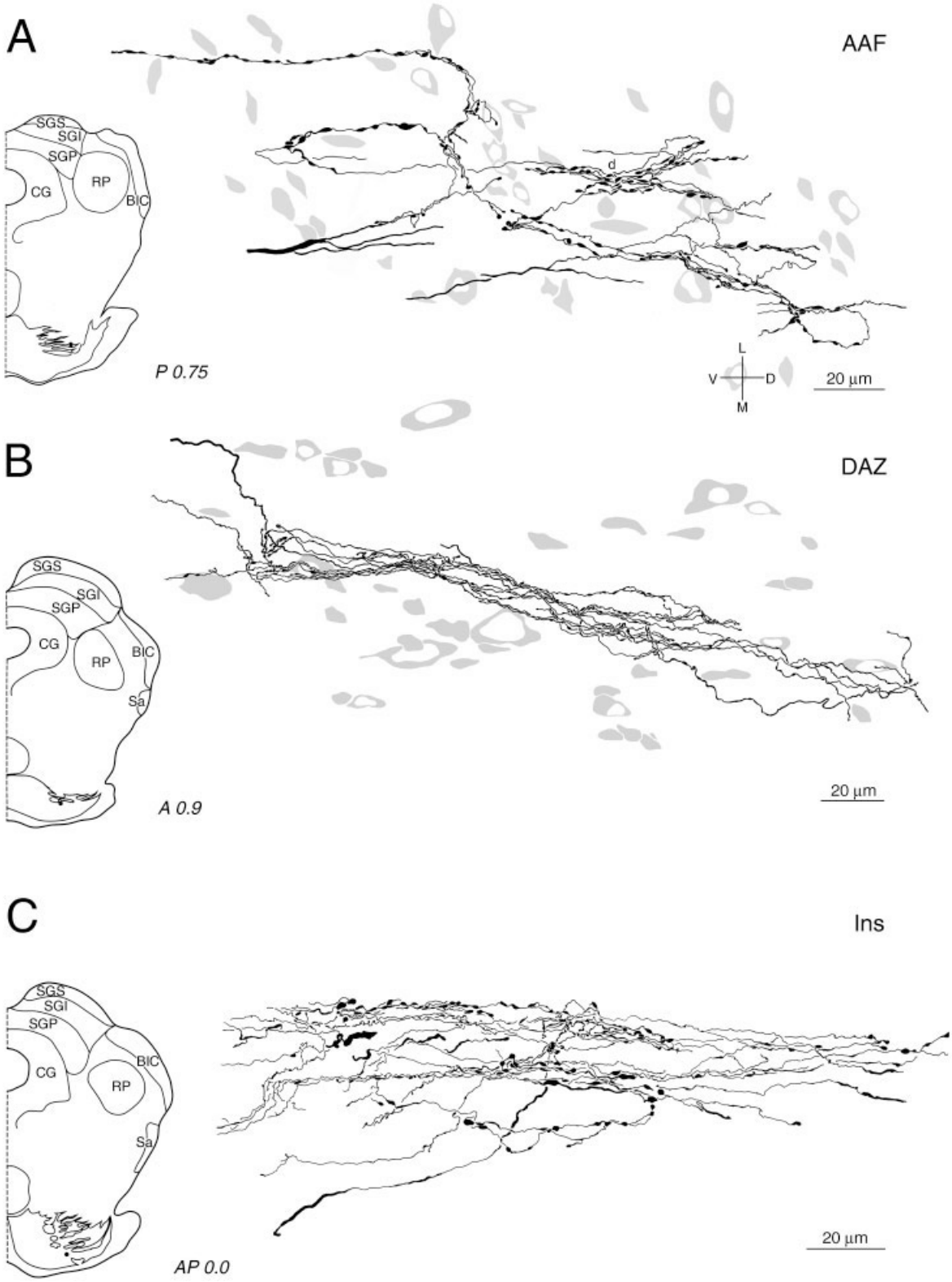

Fig. 11. BDA-filled single CP axon terminals after injections in areas AAF (**A**), DAZ (**B**), and Ins (**C**). All such preterminal fibers formed narrow fascicles with the boutons concentrated in elongated, dense masses of endings (d), mainly in the neuropil and with few terminals near perikarya, irrespective of their areal origins. This organization resembled that described for the type 2 terminal plexus.

Winer et al., 2001) and midbrain (Fig. 2C,F,I,L; Winer et al., 1998).

The morphological features of the CP terminal plexus are independent of their AC origin, but their form does reflect the particular orientation and distribution of the PN cells that they appear to target. This finding is in accord with the differential structure of corticothalamic plexuses terminating in different MGB subnuclei (Winer et al., 1999). All CP preterminal fibers ending in a region have similar morphologic characteristics; they may share a common pattern of synaptic transmission irrespective of the cortical area of origin.

Some restricted regions of AC target one pontine region exclusively. This implies that different cells in an AC area may project to different pontine regions, and the several patterns of their terminal arbors in each pontine region might underlie the transmission of different types of auditory information. Studies with multiple anterograde and retrograde tracers will be required to address this question.

Auditory CP plexuses differ from other corticofugal projections such as those targeting the cochlear nucleus (Jacomme et al., 2003), MGB (Winer et al., 1999), IC (Winer et al., 1998), claustrum (Beneyto and Prieto, 2001), and sagulum (Beneyto et al., 1998). Many of these axon terminal fields are widespread and diffuse, with sparse ramifications extending in several axes. The disposition of their boutons would require massive spatial and temporal convergence to elicit a concerted response, and, thus, they might function more as synaptic modulators than drivers. Although type I CP plexuses do not have such an architecture, they have boutons in the fiber-rich fascicles that would be ideal candidates to excite pontocerebellar neurons tonically, such that auditory input might influence muscle tone or motor planning continuously. In contrast, the larger auditory type 2 CP axons have multiple ramifications with abundant en passant boutons that form plexuses concentrated focally. This may reflect that a given small AC region targets few pontine neurons, providing a structural basis for a rapid, focal control essential for ongoing cerebellar motor coordination, reflecting a synaptic driving function. This classification of axons on the basis of their preterminal plexus is in good agreement with the postulated driver and modulator categories (Sherman and Guillery, 1998) perhaps corresponding to CP categories type 2 and type 1, respectively.

A further possibility is that the type 2 endings contribute to a discontinuous representation of characteristic frequency in cerebellar cortex that is analogous to the fractured maps reported for somatic sensory input (Shambes et al., 1978). Resolving these competing and complementary (but not necessarily mutually exclusive) hypotheses will require further electrophysiological studies in conjunction with transneuronal tract tracing methodologies. Finally, other implications may follow when the architecture of IC projections terminating in the PN (Hashikawa, 1983) is elucidated to derive a more inclusive profile of the several descending influences converging on the PN (Fig. 12).

Possible functional correlates

Auditory information reaching the cerebellum is necessary for integrating and/or translating the sensory feedforward projections to the premotor and motor areas for movement planning and execution (Kamada et al., 1992). The PN is thus a key conduit in focusing the AC projections before they reach the cerebellum.

Topographic studies found that CP neurons are dispersed throughout AC (Keizer et al., 1987). This arrangement departs from the tonotopic organization of AC and may relate to physiological findings for a discontinuous spatial map formed by isolated neurons widely distributed throughout AC, and which encodes sound source location in auditory space using a population processing strategy (Phillips and Brugge, 1985; Clarey et al., 1994; Brugge et al., 1996; Middlebrooks et al., 1998; Mickey and Middlebrooks, 2001). Such an arrangement is congruent with the diffuse organization of characteristic frequency in area AII (Schreiner and Cynader, 1984), and with the focal and mosaic nature of CP projections (present results).

From this perspective, PN physiological recordings (Aitkin and Boyd, 1978) may support the hypothesis of the preservation of an AC map of the acoustic space through the auditory CP projection. For instance, the cortical neurons forming or contributing to this map and their pontine targets share important features related to sound localization, such as the predominance of excitatory–excitatory units (Brugge et al., 1969; Aitkin and Boyd, 1978; Roth et al., 1980; Middlebrooks and Pettigrew, 1981; Rajan et al., 1990; Middlebrooks and Green, 1991; Toronchuk et al., 1992; Korte and Rauschecker, 1993; Clarey et al., 1994; Middlebrooks et al., 1998), and broad frequency tuning (Aitkin and Boyd, 1978; Middlebrooks and Green, 1991). Moreover, two other structures that contain maps of the auditory space, the lateral/external nucleus of the inferior colliculus (Aitkin and Boyd, 1978) and its avian homologue (Knudsen and Konishi, 1978; Peña, 2002), and the superior colliculus (Matsuzaki and Kyuhou, 1997), also project to the pons, thus supporting a role for spatial representation in the PN. Considering that retinotopy and somatotopy both encode spatial information, it seems logical to predict that sound source localization, rather than precise characteristic frequency tuning, would be the dominant dimension of acoustic information delivered by the PN through the CP projection, and thus enabling AC to influence premotor functions via the cerebellum.

Cytoarchitectonic implications

It has proved difficult to subdivide the PN using classical architectonic tools (Brodal and Jansen, 1946). However, territorial subdivisions exist that may be identified by their AC input patterns (Fig. 12). Thus, the lateral pontine region may be exclusively auditory, since it is apparently the sole target of AC and auditory subcortical projections (Kawamura and Brodal, 1973; Kawamura, 1975; Kandler and Herbert, 1991; Ohlrogge et al., 2001). Therefore, lateral pontine input to the cerebellum would be acoustic, with EPD as the principal source and other AC areas also projecting. In contrast, in the central and medial pons, AC projections converge with visual and somatic sensory input. This suggests that spheres of multimodal influence predate the emergence of modality-specific nuclei in phylogenetically ancient brain stem regions (Ramon-Moliner and Nauta, 1966).

The auditory and the somatic sensory CP projections end chiefly in the medial pons (Brodal, 1968a,b; Chiba, 1980; Broch-Smith and Brodal, 1990; present results), where their preterminal fibers form oblique bands. All AC areas projected to the rostral and medial pons, with AI, AII, EPI, and Te having a dense dorsolateral focus (at

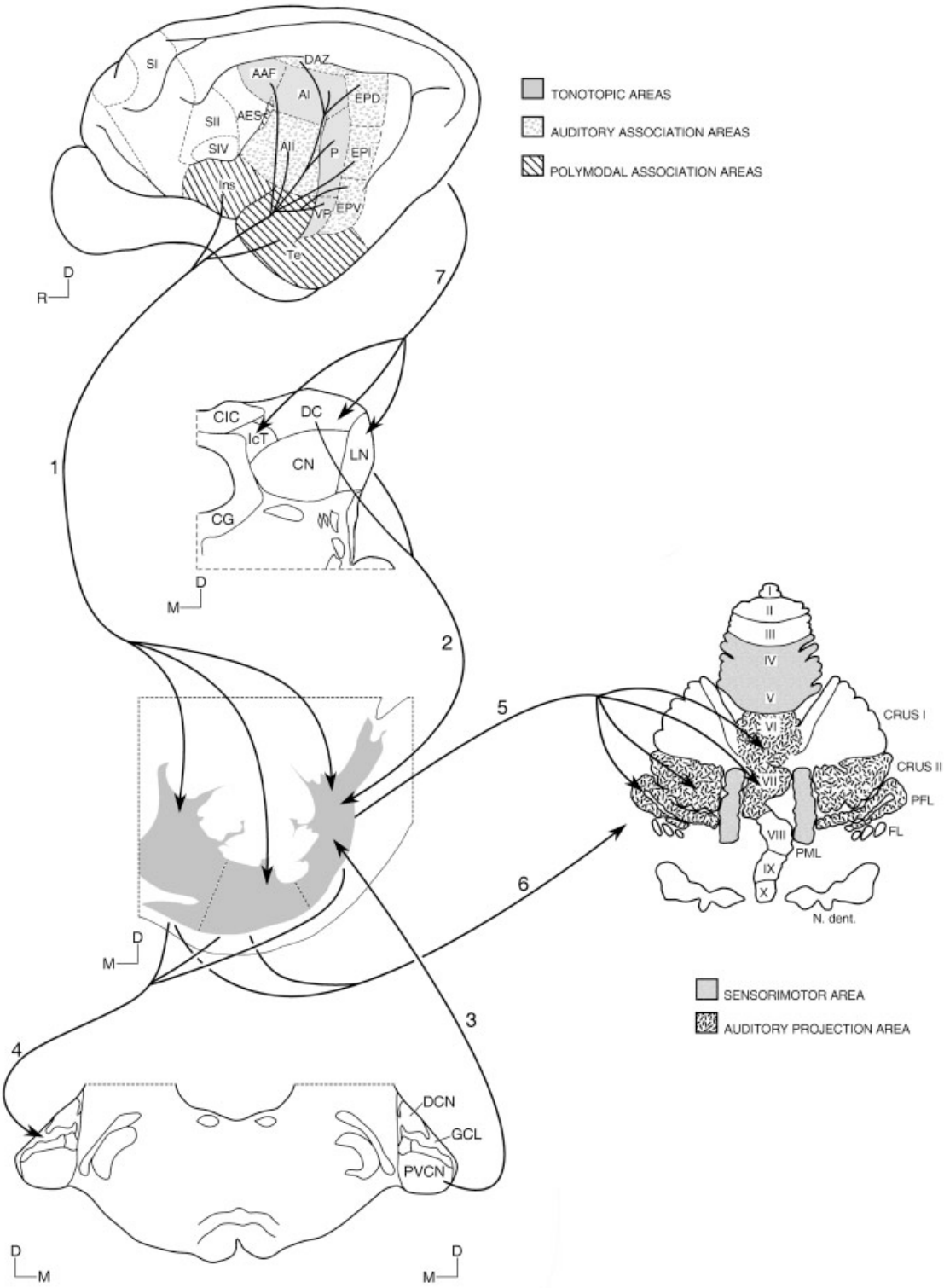

Fig. 12. Schematic of PN inputs from the AC, IC, and cochlear nucleus, and the pontine projection to the cerebellum and the cochlear nucleus. The PN receives descending inputs from all AC areas (1) that terminate in medial pons where they coincide with cortical somatosensory projections, in the central pons, a target also of cortical visual axons, and in the lateral pons, and which would be exclusively auditory. The PN also receive descending fibers from (2), the dorsal and lateral nuclei of the ipsilateral IC, and ascending input from (3), the ipsilateral posteroventral cochlear nucleus. In turn, the PN project to the contralateral cochlear nucleus granule cell domain (4), the lateral pons projects to auditory regions of the cerebellar cortex (5), while the precise target of the medial and central pons is unknown (6). Auditory inputs to the PN may be modified through indirect input to auditory centers that project to the PN, like those arising in the AC (7). The principal references for these projections are: 1) present results, 2) Aas (1989), 3) Thompson (1998), 4) Ohlrogge et al. (2001), described in rat, 5) Chiba (1980), 6) Brodal (1983), and 7) Winer et al. (1998).

~A1.0) apparently overlapping with that arising from the second somatosensory area (SII: Brodal, 1968a,b; Broch-Smith and Brodal, 1990). This implies that somatosensory and auditory information may converge and be integrated in the medial pons.

The visual cortex input targets the rostral ventral pontine region (Bjaalie and Brodal, 1989; Broch-Smith and Brodal, 1990) and thus may overlap with the auditory CP terminals from area AII (present results), perhaps ultimately to terminate in the same cerebellar region for subsequent, premotor-related actions that require multisensory integration (Aitkin and Rawson, 1983). However, our results cannot specify whether the somatosensory, visual, and auditory CP axons converge on the same postsynaptic PN neurons, or form contiguous, but synaptically independent, terminal fields and plexuses. Elucidating any proposed role of the PN as integrators of inputs from different sensory modalities will require conjoint physiological studies and tract-tracing experiments.

ACKNOWLEDGMENTS

We thank Mr. David T. Larue for superb technical assistance with histology. We thank James J. Diehl for sharing some experimental material. Dr. Mónica Beneyto generously drew early drafts of Figures 10 and 11.

LITERATURE CITED

Aas JE. 1989. Subcortical projections to the pontine nuclei in the cat. J Comp Neurol 282:331–354.

Adams JC. 1981. Heavy metal intensification of DAB-based HRP reaction product. J Histochem Cytochem 29:775.

Aitkin LM, Boyd J. 1978. Acoustic input to the lateral pontine nuclei. Hear Res 1:67–77.

Aitkin LM, Rawson JA. 1983. Frontal sound source location is represented in the cat cerebellum. Brain Res 265:317–321.

Albus K, Donate-Oliver F, Sanides D, Fries W. 1981. The distribution of pontine projection cells in visual and association cortex of the cat: an experimental study with horseradish peroxidase. J Comp Neurol 201: 175–189.

Andersen RA, Roth GL, Aitkin LM, Merzenich MM. 1980a. The efferent projections of the central nucleus and the pericentral nucleus of the inferior colliculus in the cat. J Comp Neurol 194:649–662.

Andersen RA, Snyder RL, Merzenich MM. 1980b. The topographic organization of corticocollicular projections from physiologically identified loci in AI, AII, and anterior auditory fields of the cat. J Comp Neurol 191:479–494.

Avanzini G, Manzia D, Pelliccioli G. 1969. Ascending and descending connections of the insular cortex of the cat. Arch Ital Biol 107:564–568.

Bajo VM, Rouiller EM, Welker E, Clarke S, Villa AEP, de Ribaupierre Y, de Ribaupierre F. 1995. Morphology and spatial distribution of corticothalamic terminals originating from the cat auditory cortex. Hear Res 83:161–174.

Beneyto M, Prieto JJ. 2001. Connections of the auditory cortex with the claustrum and the endopiriform nucleus in the cat. Brain Res Bull 54:485–498.

Beneyto M, Winer JA, Larue DT, Prieto JJ. 1998. Auditory connections and neurochemistry of the sagulum. J Comp Neurol 401:329–351.

Bjaalie JG. 1985. Distribution in areas 18 and 19 of neurons projecting to the pontine nuclei: a quantitative study in the cat with retrograde transport of HRP-WGA. Exp Brain Res 57:585–597.

Bjaalie JG. 1986. Distribution of CP neurons in visual areas of the middle suprasylvian sulcus: quantitative studies in the cat. Neuroscience 18: 1013–1033.

Bjaalie JG. 1989. The corticopontine projection from area 20 and surrounding areas in the cat: terminal fields and distribution of cells of origin as compared to other visual cortical areas. Neuroscience 29:81–93.

Bjaalie JG, Brodal P. 1983. Distribution in area 17 of neurons projecting to the pontine nuclei: a quantitative study in the cat with retrograde transport of HRP-WGA. J Comp Neurol 221:289–303.

Bjaalie JG, Brodal P. 1989. Visual pathways to the cerebellum: segregation in the pontine nuclei of terminal field from different visual cortical areas in the cat. Neuroscience 29:95–107.

Bjaalie JG, Diggle P. 1990. Statistical analysis of corticopontine neuron distribution in visual areas 17, 18 and 19 of the cat. J Comp Neurol 295:15–32.

Bjaalie JG, Sudbo J, Brodal P. 1997. Corticopontine terminal fibres form small scale clusters and large scale lamellae in the cat. Neuroreport 8:1651–1655.

Brandner S, Redies H. 1990. The projection of the medial geniculate body to field AI: organization in the isofrequency dimension. J Neurosci 10:50–61.

Brandt HM, Apkarian AV. 1992. Biotin-dextran: a sensitive anterograde tracer for neuroanatomic studies in rat and monkey. J Neurosci Methods 45:35–40.

Broch-Smith T, Brodal P. 1990. Organization of the cortico-pontocerebellar pathway to the dorsal paraflocculus. Arch Ital Biol 128:249–271.

Brodal P. 1968a. The corticopontine projection in the cat. Demonstration of a somatotopically organized projection from the primary sensorimotor cortex. Exp Brain Res 5:210–234.

Brodal P. 1968b. The corticopontine projection in the cat. Demonstration of a somatotopically organized projection from the second sensorimotor cortex. Arch Ital Biol 106:310–332.

Brodal P. 1972a. The corticopontine projection from the visual cortex in the cat. I. The total projection and the projection from area 17. Brain Res 39:297–317.

Brodal P. 1972b. The corticopontine projection from the visual cortex in the cat. II. The projection from areas 18 and 19. Brain Res 39:319–335.

Brodal P. 1972c. The corticopontine projection in the cat. The projection from the auditory cortex. Arch Ital Biol 110:119–144.

Brodal P. 1983. Principles of organization of the corticopontocerebellar projection to crus II in the cat with particular reference to the parietal cortical areas. Neuroscience 10:621–638.

Brodal P, Bjaalie JG. 1992. Organization of the pontine nuclei. Neurosci Res 13:83–118.

Brodal A, Jansen J. 1946. The pontocerebellar projection in the rabbit and cat. Experimental investigations. J Comp Neurol 84:31–118.

Brodal P, Steen N. 1983. The corticopontocerebellar pathway to crus I in the cat as studied with anterograde and retrograde transport of horseradish peroxidase. Brain Res 267:1–17.

Brugge JF, Dubrovsky NA, Aitkin LM, Anderson DJ. 1969. Sensitivity of single neurons in auditory cortex of cat to binaural tonal stimulation; effects of varying interaural time and intensity. J Neurophysiol 32: 1005–1024.

Brugge JF, Reale RA, Hind JE. 1996. The structure of spatial receptive fields of neurons in primary auditory cortex of the cat. J Neurosci 16:4420–4437.

Chiba M. 1980. Patterns of organization of the corticopontine projection in the cat with comments on the pontocerebellar projection. J Hirnforsch 21:89–99.

Clarey JC, Irvine DRF. 1986. Auditory response properties of neurons in the auditory ectosylvian sulcus of the cat. Brain Res 386:12–19.

Clarey JC, Irvine DRF. 1990a. The anterior ectosylvian sulcal auditory field in the cat. I. An electrophysiological study of its relationship to surrounding auditory cortical fields. J Comp Neurol 301:289–303.

Clarey JC, Irvine DRF. 1990b. The anterior ectosylvian sulcal auditory field in the cat. II. A horseradish peroxidase study of its thalamic and cortical connections. J Comp Neurol 301:304–324.

Clarey JC, Barone P, Imig TJ. 1994. Functional organization of sound direction and sound pressure level in primary auditory cortex of the cat. J Neurophysiol 72:2383–2405.

Clascá F, Llamas A, Reinoso-Suárez F. 1997. Insular cortex and neighboring fields in the cat: a redefinition based on cortical microarchitecture and connections with the thalamus. J Comp Neurol 384:456–482.

Coomes DL, Schofield BR. 2004. Projections from the auditory cortex to the superior olivary complex in guinea pigs. Eur J Neurosci 19:2188–2200.

Cooper MH, Young PA. 1976. Cortical projections to the inferior colliculus of the cat. Exp Neurol 51:488–502.

Diamond IT, Jones EG, Powell TPS. 1969. The projection of the auditory cortex upon the diencephalon and brain stem in the cat. Brain Res 15:305–340.

Fallon JH, Benevento LA. 1977. Auditory-visual interaction in cat orbital-insular cortex. Neurosci Lett 6:143–149.

Fallon JH, Benevento LA, Loe PR. 1978. Frequency-dependent inhibition to tones in neurons of cat insular cortex. Brain Res 145:161–167.

Giménez-Amaya JM. 1988. Afferent connections to the pontine nuclei from the cortex to the anterior ectosylvian sulcus in the cat. Neurosci Lett 85:29–34.

Glickstein M. 1997. Mossy-fibre sensory input to the cerebellum. Prog. Brain Res 114:251–259.

Hashikawa T. 1983. The inferior colliculopontine neurons of the cat in relation to other collicular descending neurons. J Comp Neurol 219: 241–249.

Hazama M, Kimura A, Donishi T, Sakoda T, Tamai Y. 2004. Topography of corticothalamic projections from the auditory cortex of the rat. Neuroscience 124:655–667.

He J, Hashikawa T. 1998. Connections of the dorsal zone of cat auditory cortex. J Comp Neurol 400:334–348.

Höllander H, Brodal P, Walberg F. 1969. Electronmicroscopic observations on the structure of the pontine nuclei and the mode of termination of the corticopontine fibres. An experimental study in the cat. Exp Brain Res 7:95–110.

Huang CL, Winer JA. 2000. Auditory thalamocortical projections in the cat: laminar and areal patterns of input. J Comp Neurol 427:302–331.

Imig TJ, Morel A. 1984. Topographic and cytoarchitectonic organization of thalamic neurons related to their targets in low-, middle-, and high-frequency representations in cat auditory cortex. J Comp Neurol 227: 511–539.

Imig TJ, Morel A. 1985. Tonotopic organization in lateral part of posterior group of thalamic nuclei in the cat. J Neurophysiol 53:836–851.

Jacomme AV, Nodal FR, Bajo VM, Manunta Y, Edeline JM, Babalian A, Rouiller EM. 2003. The projection from auditory cortex to cochlear nucleus in guinea pigs: an in vivo anatomical and in vitro electrophysiological study. Exp Brain Res 153:467–476.

Jen PH-S, Hou T, Wu M. 1993. Neurons in the inferior colliculus, auditory cortex and pontine nuclei of the FM bat, *Eptesicus fuscus* respond to pulse repetition rate differently. Brain Res 613:152–155.

Kamada T, Wu M, Jen PH-S. 1992. Auditory response properties and spatial response areas of single neurons in the pontine nuclei of the big brown bat, *Eptesicus fuscus*. Brain Res 575:187–198.

Kandler K, Herbert H. 1991. Auditory projections from the cochlear nucleus to pontine and mesencephalic reticular nuclei in the rat. Brain Res 562:230–242.

Kawamura K. 1975. The pontine projection from the inferior colliculus in the cat. An experimental anatomical study. Brain Res 95:309–322.

Kawamura K, Brodal A. 1973. The tectopontine projection in the cat: an experimental anatomical study with comments on pathways for teleceptive impulses to the cerebellum. J Comp Neurol 149:371–390.

Kawamura K, Chiba M. 1979. Cortical neurons projecting to the pontine nuclei in the cat. An experimental study with the horseradish peroxidase technique. Exp Brain Res 35:269–285.

Keizer K, Kuypers HG, Ronday HK. 1987. Branching cortical neurons in cat which project to the colliculi and to the pons: a retrograde fluorescent double-labeling study. Exp Brain Res 67:1–15.

Kimura A, Donishi T, Sakoda T, Hazama M, Tamai Y. 2003. Auditory thalamic nuclei projections to the temporal cortex in the rat. Neuroscience 117:1003–1016.

Knight PL. 1977. Representation of the cochlea within the anterior auditory field (AAF) of the cat. Brain Res 130:447–467.

Knowlton BJ, Thompson JK, Thompson RF. 1993. Projections from the auditory cortex to the pontine nuclei in the rabbit. Behav Brain Res 56:23–30.

Knudsen EI, Konishi M. 1978. A neural map of auditory space in the owl. Science 200:795–797.

Korte M, Rauschecker JP. 1993. Auditory spatial tuning of cortical neurons is sharpened in cats with early blindness. J Neurophysiol 70:1717–1721.

Kusama T, Otani K, Kawana E. 1966. Projections of the motor, somatic sensory, auditory and visual cortices in cats. Prog Brain Res 21:292–322.

Lee HS, Mihailoff GA. 1990. Convergence of cortical and cerebellar projections on single basilar pontine neurons: a light and electron microscopic study in the rat. Neuroscience 39:561–577.

Leergaard TB. 2003. Clustered and laminar topographic patterns in rat cerebro-pontine pathways. Anat Embryol (Berl) 206:149–162.

Leergaard TB, Lakke EA, Bjaalie JG. 1995. Topographical organization in the early postnatal corticopontine projection: a carbocyanine dye and 3-D computer reconstruction study in the rat. J Comp Neurol 361:77–94.

Leergaard TB, Lyngstad KA, Thompson JH, Taeymans S, Vos BP, De Schutter E, Bower JM, Bjaalie JG. 2000. Rat somatosensory cerebropontocerebellar pathways: spatial relationships of the somatotopic map of the primary somatosensory cortex are preserved in a three-dimensional clustered pontine map. J Comp Neurol 422:246–266.

Legg CR, Mercier B, Glickstein M. 1989. Corticopontine projection in the rat: the distribution of labelled cortical cells after large injections of horseradish peroxidase in the pontine nuclei. J Comp Neurol 286:427–441.

Matsuzaki R, Kyuhou S. 1997. Pontine neurons which relay projections from the superior colliculus to the posterior vermis of the cerebellum in the cat: distribution and visual properties. Neurosci Lett 236:99–102.

Merzenich MM, Knight PL, Roth GL. 1975. Representation of cochlea within primary auditory cortex. J Neurophysiol 38:231–249.

Mesulam MM. 1978. Tetramethyl benzidine for horseradish peroxidase neurohistochemistry: a non-carcinogenic blue reaction product with superior sensitivity for visualizing neural afferents and efferents. J Histochem Cytochem 26:106–117.

Mickey BJ, Middlebrooks JC. 2001. Responses of auditory cortical neurons to pairs of sounds: correlates of fusion and localization. J Neurophysiol 86:1333–1350.

Middlebrooks JC, Green DM. 1991. Sound localization by human listeners. Annu Rev Psychol 42:135–159.

Middlebrooks JC, Pettigrew JD. 1981. Functional classes of neurons in primary auditory cortex of the cat distinguished by sensitivity to sound location. J Neurosci 1:107–120.

Middlebrooks JC, Xu L, Eddins AC, Green DM. 1998. Codes for sound-source location in nontonotopic auditory cortex. J Neurophysiol 80: 863–881.

Mihailoff GA, Bourell KW. 1986. Synapse formation and other ultrastructural features of postnatal development in the basilar pontine nuclei of the rat. Dev Brain Res 28:195–212.

Mihailoff GA, King JS. 1975. The basilar pontine gray of the opossum: a correlated light and electron microscopic analysis. J Comp Neurol 159:521–552.

Mihailoff GA, Burne RA, Woodward DJ. 1978. Projections of the sensorimotor cortex to the basilar pontine nuclei in the rat: an autoradiographic study. Brain Res 145:347–354.

Mihailoff GA, Adams CE, Woodward DJ. 1984. An autoradiographic study of the postnatal development of sensorimotor and visual components of the corticopontine system. J Comp Neurol 222:116–127.

Morel A, Imig TJ. 1987. Thalamic projections to fields A, AI, P, and VP in the cat auditory cortex. J Comp Neurol 265:119–144.

Niimi K, Matsuoka H. 1979. Thalamocortical organization of the auditory system in the cat studied by retrograde axonal transport of horseradish peroxidase. Adv Anat Embryol Cell Biol 57:1–56.

Ohlrogge M, Doucet JR, Ryugo DK. 2001. Projections of the pontine nuclei to the cochlear nucleus in rats. J Comp Neurol 436:290–303.

Overby SE, Bjaalie JG, Brodal P. 1989. Uneven densities of corticopontine neurons in the somatosensory cortex: a quantitative experimental study in the cat. Exp Brain Res 77:653–665.

Peña JL. 2002. Neurons that encode sound direction. Rev Neurol 34:265–271.

Phillips DP, Brugge JF. 1985. Progress in neurophysiology of sound localization. Annu Rev Psychol 36:245–274.

Phillips DP, Irvine DRF. 1982. Properties of single neurons in the anterior auditory field (AAF) of cat cerebral cortex. Brain Res 248:237–244.

Phillips DP, Orman SS. 1984. Responses of single neurons in posterior field of cat auditory cortex to tonal stimulation. J Neurophysiol 51:147–163.

Qian Y, Jen PH-S. 1994. Fos-like immunoreactivity elicited by sound stimulation in the auditory neurons of the big brown bat *Eptesicus fuscus*. Brain Res 664:241–246.

Rajan R, Aitkin LM, Irvine DRF, McKay J. 1990. Azimuthal sensitivity of neurons in primary auditory cortex of cats. I. Types of sensitivity and the effects of variations in stimulus parameters. J Neurophysiol 64: 872–887.

Ramon-Moliner E, Nauta WJH. 1966. The isodendritic core of the brain stem. J Comp Neurol 126:311–335.

Reale RA, Imig TJ. 1980. Tonotopic organization in auditory cortex of the cat. J Comp Neurol 182:265–291.

Reale RA, Imig TJ. 1983. Auditory cortical field projections to the basal ganglia of the cat. Neuroscience 8:67–86.

Roda JM, Reinoso-Suarez F. 1983. Topographical organization of the thalamic projections to the cortex of the anterior ectosylvian sulcus in the cat. Exp Brain Res 49:131–139.

Roth GL, Kochhar RK, Hind JE. 1980. Interaural time differences: implications regarding the neurophysiology of sound localization. J Acoust Soc Am 68:1643–1651.

Rouiller EM, de Ribaupierre F. 1990. Arborization of corticothalamic axons in the auditory thalamus of the cat: a PHA-L tracing study. Neurosci Lett 108:29–35.

Rouiller EM, Hornung JP, de Ribaupierre F. 1989. Extrathalamic ascending projections to physiologically identified fields of the cat auditory cortex. Hear Res 40:233–246.

Schmahmann JD, Pandya DN. 1991. Projections to the basis pontis from the superior temporal sulcus and superior temporal region in the rhesus monkey. J Comp Neurol 308:224–248.

Schofield BR, Coomes DL. 2005. Projections from auditory cortex contact cells in the cochlear nucleus that project to the inferior colliculus. Hear Res 206:3–11.

Schreiner CE, Cynader MS. 1984. Basic functional organization of second auditory cortical field (AII) of the cat. J Neurophysiol 51:1284–1305.

Schuller G, Covey E, Casseday JH. 1991. Auditory pontine grey: connections and response properties in the horseshoe bat. Eur J Neurosci 3:648–662.

Shambes GM, Gibson JM, Welker W. 1978. Fractured somatotopy in granule cell tactile areas of rat cerebellar hemispheres revealed by micromapping. Brain Behav Evol 15:94–140.

Sherman SM, Guillery RW. 1998. On the actions that one nerve cell can have on another: distinguishing "drivers" from "modulators." Proc Natl Acad Sci U S A 95:7121–7126.

Shinonaga Y, Takada M, Mizuno N. 1994. Direct projections from the non-laminated divisions of the medial geniculate nucleus to the temporal polar cortex and amygdala in the cat. J Comp Neurol 340:405–426.

Sindberg RM, Thompson RF. 1962. Auditory response fields in ventral temporal and insular cortex in cat. J Neurophysiol 25:21–28.

Suga N, Gao E, Zhang Y, Ma X, Olsen JF. 2000. The corticofugal system for hearing: recent progress. Proc Natl Acad Sci U S A 97:11807–11814.

Thompson AM. 1998. Heterogeneous projections of the cat posteroventral cochlear nucleus. J Comp Neurol 390:439–453.

Toronchuk JM, Stumpf E, Cynader MS. 1992. Auditory cortex neurons sensitive to correlates of auditory motion: underlying mechanisms. Exp Brain Res 88:169–180.

Vischer MW, Hausler R, Rouiller EM. 1994. Distribution of Fos-like immunoreactivity in the auditory pathway of the Sprague-Dawley rat elicited by cochlear electrical stimulation. Neurosci Res 19:175–185.

Weedman DL, Ryugo DK. 1996. Projections from auditory cortex to the cochlear nucleus in rats: synapses on granule cell dendrites. J Comp Neurol 371:311–324.

Wiesendanger R, Wiesendanger M. 1982a. The corticopontine system in the rat. I. Mapping of corticopontine neurons. J Comp Neurol 208:215–226.

Wiesendanger R, Wiesendanger M. 1982b. The corticopontine system in the rat. II. The projection pattern. J Comp Neurol 208:227–238.

Winer JA. 1992. The functional architecture of the medial geniculate body and the primary auditory cortex. In: Webster DB, Popper AN, Fay RR, editors. Springer handbook of auditory research, vol. 1. The mammalian auditory pathway: neuroanatomy. New York: Springer. p 222–409.

Winer JA, Larue DT, Diehl JJ, Hefti BJ. 1998. Auditory cortical projections to the cat inferior colliculus. J Comp Neurol 400:147–174.

Winer JA, Larue DT, Huang CL. 1999. Two systems of giant axon terminals in the cat medial geniculate body: convergence of cortical and GABAergic inputs. J Comp Neurol 413:181–197.

Winer JA, Diehl JJ, Larue DT. 2001. Projections of auditory cortex to the medial geniculate body of the cat. J Comp Neurol 430:27–55.

Woolsey CN. 1960. Organization of cortical auditory system: a review and synthesis. In: Rasmussen GL, Windle WF, editors. Neural mechanisms of the auditory and vestibular systems. Springfield, IL: CC Thomas. p 165–180.

Woolsey CN. 1961. Organization of cortical auditory system. In: Rosenblith WA, editor. Sensory communication. Cambridge, MA: MIT Press. p 235–257.

Wu MI, Jen PH-S. 1995. Responses of pontine neurons of the big brown bat, *Eptesicus fuscus*, to temporally patterned sound pulses. Hear Res 85: 155–168.

Xiao Z, Suga N. 2002. Modulation of cochlear hair cells by the auditory cortex in the mustached bat. Nat Neurosci 5:57–63.

Yan J, Ehret G. 2001. Corticofugal reorganization of the midbrain tonotopic map in mice. Neuroreport 12:3313–3316.